ASNC IMAGING GUIDELINES FOR NUCLEAR CARDIOLOGY PROCEDURES

Single photon-emission computed tomography

Thomas A. Holly, MD,[a] Brian G. Abbott, MD,[b] Mouaz Al-Mallah, MD,[c] Dennis A. Calnon, MD,[d] Mylan C. Cohen, MD, MPH,[e] Frank P. DiFilippo, PhD,[f] Edward P. Ficaro, PhD,[g] Michael R. Freeman, MD,[h] Robert C. Hendel, MD,[i] Diwakar Jain, MD,[j] Scott M. Leonard, MS, CNMT, RT(N),[a] Kenneth J. Nichols, PhD,[k] Donna M. Polk, MD, MPH,[l] and Prem Soman, MD, PhD[m]

1. INTRODUCTION

The current document is an update of an earlier version of single photon emission tomography (SPECT) guidelines that was developed by the American Society of Nuclear Cardiology. Although that document was only published a few years ago, there have been significant advances in camera technology, imaging protocols, and reconstruction algorithms that prompted the need for a revised document. This publication is designed to provide imaging guidelines for physicians and technologists who are qualified to practice nuclear cardiology. While the information supplied in this document has been carefully reviewed by experts in the field, the document should not be considered medical advice or a professional service. We are cognizant that SPECT technology is evolving rapidly and that these recommendations may need further revision in the near future. Hence, the imaging guidelines described in this publication should not be used in clinical studies until they have been reviewed and approved by qualified physicians and technologists from their own particular institutions.

From Northwestern University,[a] Chicago, IL; Warren Alpert Medical School of Brown University,[b] Providence, RI; Henry Ford Hospital,[c] Detroit, MI; MidOhio Cardiology & Vascular Consultants,[d] Columbus, OH; Maine Cardiology Associates,[e] South Portland, ME; Cleveland Clinic,[f] Cleveland, OH; University of Michigan,[g] Ann Arbor, MI; St. Michael's Hospital,[h] University of Toronto, Toronto, ON; University of Miami Miller School of Medicine,[i] Miami, FL; Drexel University College of Medicine,[j] Newton Square, PA; Long Island Jewish Medical Center,[k] New Hyde Park, NY; Hartford Hospital,[l] Hartford, CT; UPMC Cardiovascular Institute,[m] Pittsburgh, PA.

Unless reaffirmed, retired, or amended by express action of the Board of Directors of the American Society of Nuclear Cardiology, this Imaging Guideline shall expire as of May 2015.

Reprint requests: Thomas A. Holly, MD, Northwestern University, Chicago, IL.

J Nucl Cardiol
1071-3581/$34.00

doi:10.1007/s12350-010-9246-y

2. INSTRUMENTATION QUALITY ASSURANCE AND PERFORMANCE

The proper choice of equipment to acquire clinical data and a well-designed quality assurance (QA) program are both essential requirements for optimizing diagnostic accuracy and ensuring consistent, high-quality imaging. The following guidelines are intended to provide an appropriate means of assessing equipment function in conjunction with nuclear cardiology imaging. Because the optimal manner in which to perform specific tests varies considerably between models of imaging equipment, this document is not intended to replace manufacturers' recommendations.

For decades, the design of SPECT cameras has remained essentially unchanged, consisting of one or more large-area scintillation or Anger cameras [single NaI(Tl) crystal with large photomultiplier tubes (PMTs) and parallel-hole collimator]. The QA and performance of these cameras are well understood, and detailed guidelines are presented in this document. However, in recent years, novel and dedicated cardiac SPECT cameras have emerged with significantly different detector, collimator, and system designs. Because this technology is rapidly evolving, detailed guidelines for QA testing do not yet exist for these new designs. Until detailed guidelines become available, the user is responsible for assessing and following vendor recommendations, and must devise acceptable QA standards specific to the scanner design. To assist in this endeavor, the basic design concepts and their implications on performance and QA are summarized in this document.

2.1. Detectors

Detectors are the heart of a SPECT system and are responsible for collecting the high-energy photons emitted by the patient, estimating the photon energy and location of interaction, and generating count data for subsequent image reconstruction. The ability to perform these duties depends on their design, materials, and electronics. Energy resolution, camera sensitivity, and

Published online: 15 June 2010

spatial resolution are the primary variables that dictate the performance of a SPECT detector.

2.1.1. Scintillation camera (anger camera). The majority of SPECT systems are based on Anger camera technology where one or more cameras rotate about the body of the patient. Anger cameras consist of a single crystal, which absorbs incident gamma photons and scintillates or emits light in response, and in back of which are banks of photomultiplier tubes and electronics to compute gamma ray energy and the location of scintillation within the crystal. Anger camera NaI(Tl) crystals are typically 1/4 to 3/8 in. thick, although they may be as thick as 5/8 in. The thicker the crystal, the greater the sensitivity of the Anger camera, because of the increased probability that a gamma ray passing through the crystal will interact. However, the thicker the crystal, the greater the spread of the emitted light photons produced from the scintillation, and the less precise the computation of gamma ray interaction location resulting in poorer intrinsic resolution of the camera.

2.1.2. Scintillation crystals (pixelated). An array of scintillation crystals is an alternative to the single-crystal Anger camera design. A large number of small crystals (e.g., 6 mm CsI(Tl) cubes) are coated with reflective material and packed into an array. An advantage of this pixelated design is that the scintillation light is much more focused than in an Anger camera and can be detected by a photodiode array instead of conventional PMTs, thereby making the detector much more compact. A possible concern for pixelated detectors is that their less efficient light collection may degrade energy resolution. Pixelated detectors are capable of very high counting rates due to their isolated light pulses and have been used in first-pass cardiac scintigraphy.

2.1.3. Semiconductor/solid-state detectors. Recently, alternative SPECT systems have been introduced, some based on small solid-state detector modules. In solid-state detectors, gamma rays are absorbed into the semiconductor material which directly generates electron-hole pairs which are pulled to the end plates through an applied electric field. The collected charge from the electron-hole pair is used to determine the location and energy of the gamma ray. One such solid-state detector is made of cadmium zinc telluride (CZT), and SPECT devices utilizing these detectors have been reported to provide improved count sensitivity, superior energy resolution, and finer spatial resolution.[1,2] The magnitude of improvement that has been reported consists of simultaneously acquiring three to ten times more counts,[3] with over two times better spatial resolution than the Anger camera.[2] The small size of solid-state modules has made a number of innovative detector designs possible. Some devices now have static arrangements of CZT crystals, and the only moving part is a collimator array. Other arrangements of CZT detectors have each detector module equipped with its own pinhole collimator, for which there are no moving parts other than a mechanism to move the detector as close as possible to the patient.

2.2. Energy Resolution

Image quality is affected by energy resolution. Ideally, images would be comprised of only primary photons emitted by the decay of a radionuclide, not the secondary scattered photons. The better the energy resolution of an imaging device, the more successful the discrimination of primary from scattered photons, and thus, the better the image contrast and the more accurate quantitation of the amount and distribution of the radionuclide in vivo. In the context of myocardial perfusion imaging, systems with better energy resolution have the ability to discriminate areas of hypoperfusion from those of neighboring normal perfusion through enhanced image contrast.

A symmetric energy window of 20% centered around the 140 keV energy peak of the emitted photons is standard for Tc-99m. With the improved energy resolution of many modern cameras, a 15% window can be used with little loss of primary gamma rays, with some improvement in image contrast. The lower energy and greater width of the Tl-201 photopeak require a wider energy window. An energy window setting of 30% is appropriate for the 70 keV peak of Tl-201, and a 15% energy window is appropriate for the 167-keV peak. The absolute energy calibration can be unreliable at the low energy of Tl-201, falling at slightly different energy positions in the spectrum of different cameras. Thus, energy peak and window settings should be established for each individual camera based on the energy spectrum display.[4] For most modem Anger cameras, the energy resolution is expected to be 9-10% for the 140-keV photons from Tc-99m, and 15-17% for the 72-keV photons from Tl-201.[5] For CZT detectors, an energy resolution of 5 to 6% has been reported for Tc-99m.[1,2]

2.3. Spatial Resolution

Spatial resolution quantifies the size of the smallest object that can be resolved reliably, and is often expressed as the full-width at half-maximum (FWHM) of a point spread function. For projection data acquired with an Anger camera, the total resolution depends on the intrinsic resolution and the collimator resolution. The intrinsic resolution is typically 3.5-4.0 mm for Tc-99m and is a function of the crystal and the position

logic circuitry used to compute the location of the detected photon. The collimator has the largest impact on the spatial resolution. For a high resolution collimator, the spatial resolution is typically $\sim$10 mm for a Tc-99m point source placed at 10 cm from the collimator face. The resolution varies for different collimators depending the length and diameter of the collimator holes. Collimators with smaller and longer holes will have better spatial resolution but will have lower sensitivity.

For all SPECT imaging devices, system spatial resolution is also influenced by the image reconstruction process. The most commonly used reconstruction algorithm is filtered backprojection which involves a reconstruction kernel (e.g., a ramp function in the spatial frequency domain) and a postfilter which is usually designed to suppress image noise. In the spatial frequency domain representation, a noise smoothing filter has a high frequency roll-off whose effect is to suppress high-frequency image noise especially for count-poor studies at the expense of sacrificing spatial resolution. A roll-off at higher spatial frequency results in better spatial resolution, but often entailed images of a higher noise or lower signal-to-noise ratio.[6] Recently, more sophisticated algorithms have been employed for image reconstructions that model the physics and characteristics of the imaging system involved in the image formation process. These include the statistical maximum-likelihood expectation-maximization (ML-EM) algorithms,[7] and the ordered-subset expectation-maximization (OS-EM) algorithms.[8]

For new detector designs based on multiple small solid-state detectors, tomogram formation is implemented through the use of ML-EM or OS-EM algorithms that not only generate the tomogram, but also make it possible to correct for estimated amounts of scattered radiation, using information in multiple energy windows.[9,10] Furthermore, MLEM and OSEM algorithms enable incorporation of detailed knowledge about the manner in which detector response varies with the distance away from each detector.[11] These algorithms also enable attenuation compensation using attenuation maps obtained from scanning line sources or CT images in modem SPECT/CT system.

2.4. Detector Sensitivity

The image quality of scintigrams is largely determined by the signal-to-noise ratio. The greater the sensitivity of the device, the more counts are available, and the higher the signal-to-noise ratio. The greater the number of counts that can be acquired, the more certain one can be as to the correct three-dimensional (3D) distribution of count concentrations within the body. The amount of radionuclide that can be injected per study is limited by the amount of radiation to which the patient can be exposed during a diagnostic procedure. Thus, given that there is an upper limit to the amount of an isotope that can be injected routinely, it is desirable to have the most sensitive device available to form the clinical images.

2.5. Count Rate Limitations

At very high photon detection rates, the camera electronics can have difficulty analyzing every photon. The missed counts, often referred as dead time effects, can affect the estimated distribution of the radiotracer in the body. For current cardiac radiotracers, protocols and imaging systems, dead time effects are not an issue.

2.6. Collimation

SPECT image reconstruction requires that the incident direction of each acquired count be known. An external collimator is used to do so, by absorbing photons outside a range of incident angles as specified by the collimator design. By limiting the number of detected photons to a specific direction or small range of directions, the collimator allows the detection of only a very small fraction of the photons emitted by the patient (see Table 1). However, since a range of incident angles is allowed to pass through the collimator, there is a loss of resolution. An inherent trade-off in the design of

Table 1. Typical performance parameters for low-energy (<150 keV) collimators

Collimator type	Resolution (FWHM at 10 cm)	Efficiency	Relative efficiency
Ultra-high resolution	6.0 mm	$.5 \times 10^{-4}$	.3
High resolution	7.8 mm	1×10^{-4}	.6
All/general purpose	9.3 mm	1.7×10^{-4}	1*
High sensitivity	13.2 mm	3.5×10^{-4}	2.1

Note: A relative efficiency of 1 corresponds approximately to a collimator efficiency of 1.7×10^{-4}, whereas efficiency is defined as the fraction of gamma rays and x-rays passing through the collimator per gamma ray and x-ray emitted by the source.

SPECT collimators is resolution vs sensitivity. It is possible to improve the spatial resolution of a collimator by further restricting the range of incident angles, but this is at the expense of reducing sensitivity. Anger cameras require collimators to localize the site within the patient from which the gamma ray photons are emitted.

Because of this resolution vs sensitivity trade-off, the collimator is perhaps the most significant component of the SPECT camera affecting image quality. Most SPECT cameras for nuclear cardiology utilize conventional parallel-hole collimation. However, it has long been recognized that significant improvements in SPECT performance are possible with alternative collimator designs. Coupled with advances in detector and computing technology in recent years, new collimator designs have become practical for nuclear cardiology.

2.6.1. Parallel-hole collimation. The structure of a parallel-hole collimator is similar to that of a honeycomb, consisting of a large number of narrow channels separated by thin septa. The range of incident angles passing through the collimator depends on the channel width and length. The septa must be thick enough to absorb photons of the desired energy in order the accept photons that are incident on the collimator within a range of directions. Collimators are often categorized as low-, medium-, or high-energy depending on the photon energy for which the collimator is designed. Various designs of low-energy collimators are classified as high-resolution, all-purpose, high-sensitivity, etc., depending on the collimator's angle of incidence.

For Anger cameras, parallel-hole collimation is standard. The low-energy, high-resolution collimator is usually best for Tc-99m, although some ''all-purpose'' collimators give excellent results. Imaging with Tl-201 is usually best with the low-energy, medium-resolution (all-purpose) collimators because count statistics become limiting when using high-resolution collimators. The difference in medium- and high-resolution collimators is usually that the collimator depth (i.e., length of the collimator hole) is greater in high-resolution collimators. Medium- and high-resolution collimators have similar near-field resolution, but high-resolution collimators maintain good resolution at a greater distance from the collimator face. The difference is more important in SPECT imaging, where the distance from patient to collimator is greater.[5]

The selection of which collimator to use is important to resultant image quality. A confounding aspect of this selection is that collimators with the same name (e.g., ''general purpose'') vary in performance from one manufacturer to another. Table 1 gives approximate values for collimator specifications. The user should refer to specific imaging protocols for appropriate collimator selection. It is important to perform periodic assessment of collimator integrity, as failure to detect and correct for localized reduced sensitivity can generate uniformity-related artifacts, including reconstruction artifacts.[12,13]

The trend is to trade off some of the additional counts that would be obtained with multiple detectors equipped with general-purpose collimators for higher-resolution imaging by using higher-resolution collimators. For newer reconstruction algorithms that model the collimator blur, some degree of resolution recovery is feasible. With such algorithms, the all-purpose collimator may offer improved image quality.[14] Depending on the scanner configuration, reconstruction algorithm, radionuclide dose, and patient population, the optimal collimator choice may vary between laboratories.

2.6.2. Sweeping parallel-hole collimation. A variant of the standard parallel-hole collimator is a sweeping configuration, where an array of small detectors is arranged around the patient instead of one to three large-area Anger cameras. Each small detector is configured with a parallel-hole collimator, which restricts its field-of-view (FOV) over a small volume. To view the entire patient, each detector pivots about its own axis, sweeping its FOV like a searchlight across the entire imaging volume. With a sufficient number of these small pivoting detectors, a sufficient degree of angular sampling is achieved to reconstruct high-quality images. The sweeping FOV of the pivoting detectors provides the flexibility to control the amount of time that is spent imaging regions of the imaging FOV. By spending more time imaging the myocardium and less time imaging the rest of the chest, data collection is more efficient and could lead to reduced scan time or dose. Although the concept of sweeping parallel-hole collimation is not new,[15] recent advances in detector design have led to its practical implementation.[16] With solid-state CZT detectors, a compact stationary scanner design is feasible.

2.6.3. Converging collimation (fixed and variable fan and conebeam). With large-area Anger cameras and parallel-hole collimation, only a small fraction of the detector area is utilized in imaging the myocardium. Converging collimators allow more of the crystal area to be used in imaging the heart, magnifying the image, and increasing sensitivity.[5] Converging collimators with a short fixed focal distance have the potential for truncating portions of the heart and/or chest, especially in large patients. This truncation may generate artifacts. Currently, there is a limited clinical use of fixed-focus fan beam and cone beam collimators in nuclear cardiology.

Another converging collimator design that has reached a commercial stage is the variable-focus cone-

beam collimator.[17] The center of this collimator focuses on the heart to increase the myocardial counts acquired. The remainder of the collimator has longer focal length to improve data sampling over the entire chest and thereby reduces truncation artifact.

2.6.4. Multi-pinhole collimation. Collimation requires the mapping of a point on the detector to an angle of incidence. Conventional parallel-hole and converging hole collimators use an array of narrow channels of radiation-absorbing material to specify the angle of incidence. A fundamentally different approach is pinhole collimation where a small pinhole aperture surrounded by radiation-absorbing material allows photons to pass through. The line connecting the point of emission of the gamma photon and the pinhole aperture specifies the direction of photon incidence on the detector.

The sensitivity and resolution characteristics of pinhole collimators differ markedly from those of parallel-hole collimation. The sensitivity of a parallel-hole collimator is almost constant as a function of distance from the collimator. However, the sensitivity of a pinhole collimator depends on the inverse square of the distance from the pinhole aperture and becomes quite large at small distances. It also increases as the square of the pinhole diameter with concurrent loss in spatial resolution. The magnification factor of a pinhole is determined by the ratio of the pinhole-to-detector distance relative to the pinhole-to-source distance. With increased magnification factors, the detector intrinsic resolution has decreased effect on the total system spatial resolution which approaches that of the pinhole collimator. In summary, a pinhole collimator is most effective for imaging a small object placed close to the pinhole aperture, and is clinically used most often for thyroid imaging. Pinhole collimators have received much attention recently for small animal SPECT imaging. Multi-pinhole collimators are effective in increasing the sensitivity and angular sampling, provided that the of overlapping pinhole projections are avoided through inter-pinhole shielding, or in cases with small amount of overlap, special image reconstruction algorithms are used to minimize the effect on image quality.

Multi-pinhole collimation was used in the early days of nuclear cardiology to provide multiple angular views (and in some cases, limited angle tomography) of the myocardium.[18] With advances in iterative image reconstruction, multi-pinhole collimators have made a come-back in nuclear cardiology. Fully tomographic myocardial SPECT imaging has been demonstrated using multi-pinhole collimators with both Anger cameras[19] and small area CZT detectors.[20] The characteristics of pinhole collimation offer the potential of both improved spatial resolution and sensitivity compared to conventional pinhole collimation with Anger cameras.

2.7. System Design

The sections above have discussed the various types of detectors and collimators used in nuclear cardiology. The SPECT imaging system is built around these components to optimize the imaging protocols, patient handling, and flexibility of the scanner and the overall image quality. A complete understanding of the system design is necessary to establish a proper QA program.

2.7.1. Multi-purpose SPECT. A common system design for cardiac SPECT is a multi-purpose SPECT scanner with one or more large-area Anger cameras. The detectors are attached to a gantry which rotates the Anger cameras and adjusts their distance relative to the center-of-rotation. Projection images are acquired as the gantry rotates the detectors in a continuous or step-and-shoot mode. An advantage of this SPECT system design is that it is compatible with general nuclear medicine scans (planar and SPECT) as well as cardiac SPECT.

Single-head cameras were used widely for cardiac imaging initially. Adding more detectors is beneficial, since doubling the number of detectors doubles the acquired counts, if all other variables remain fixed. For cardiac SPECT studies in which a 180-degree orbit (right anterior oblique [RAO] to left posterior oblique [LPO] or LPO to RAO) is recommended, the preferred configuration is to have two detectors separated by 90° as they rotate around the heart. A potential concern with the 90° configuration is whether there is truncation of the SPECT projections in the region between the two detectors. Many dual-detector systems also offer a more acute configuration (e.g., 80°) and a longer scan range (e.g., 100°) to avoid possible truncation near the heart.

The various mechanical configurations and detector motions of multi-purpose SPECT systems have the potential for misalignment errors and must be included in the laboratory's QA program (e.g., center-of-rotation [COR] correction, multi-detector registration).

2.7.2. Dedicated cardiac. As nuclear cardiology grew in volume, the market expanded for SPECT scanners designed solely for cardiac imaging instead of for all nuclear medicine procedures. Many scanners emerged with smaller-area Anger camera detectors in a fixed 90° configuration, with significantly reduced cost, weight, and space requirements. However, care in patient positioning is more critical when using these dedicated cardiac SPECT systems than the multi-purpose SPECT systems with large-area detectors, to avoid truncating the heart and the associated artifacts. Otherwise, QA is similar to the multi-purpose SPECT systems.

The growth of dedicated cardiac SPECT systems also led to the adoption of novel detector and collimation technologies as described above. Because of the wide variety of designs and their novelty, their QA requirements may differ from the standard Anger camera with parallel-hole collimation. Thus a detailed quality assurance summary for each design is not presented in this document, though areas where the QA or performance may differ are noted. Each laboratory should understand these differences and consult with the vendor's user manuals to develop its own program until such standards and guidelines are developed.

2.7.3. Patient configuration. Because of the variety in SPECT scanner designs, the patient handling system can differ markedly between SPECT scanners. Although this does not impact camera quality assurance directly, the differences in patient configuration and the potential effect on study interpretation should be understood.

The conventional patient handling system holds the patient horizontally on a level table as the detectors rotate around the patient. The patient typically is imaged in a supine position, although some laboratories routinely image in the prone position.[21] Some dedicated cardiac SPECT systems instead hold the patient in a reclined position or upright position. The different direction of gravity relative to the patient may affect the expected patterns of attenuation and the degree and nature of patient motion.

Some new dedicated cardiac systems have detectors and/or collimators that move internally to the scanner and have no visible moving components. Other systems may not require detector or collimator motion at all and are entirely stationary. However, some dedicated cardiac SPECT cameras differ in that the detectors are stationary and that the patient is rotated in the upright position. The rotating chair of these cameras must be included in a center-of-rotation assessment of the QA program.

2.7.4. Data sampling. A range of angular projection images is needed to reconstruct tomographic images. The way that SPECT systems acquire the multiple projection images differs significantly. For conventional parallel-hole collimators and Anger cameras or similar detectors, recommended guidelines exist for the minimum number of angular samples.

For other designs, the topic of data sampling may not be so straightforward. Truncation with small FOV detectors may cause artifacts particularly at the edge of the FOV. Cone-beam and pinhole geometries have less data completeness at distance further away from the central transaxial image slice and show increased image artifacts. Some focused collimator designs may have sufficient sampling in the cardiac region though not over the rest of the torso. Proper patient positioning is important to ensure that the heart is in the fully sampled region.

Although each vendor has recommended cardiac imaging protocols for their cameras, the user should validate these protocols for their own use with QA phantoms if similar validation work has not yet been published. Studies with a full-scale anthropomorphic phantom would be appropriate for this validation to simulate imaging under actual conditions.

2.7.5. SPECT systems with photon sources for attenuation correction (AC). Currently, there are two types of transmission tomographic imaging systems for acquiring patient-specific attenuation maps that can be used to correct SPECT images for photon attenuation. The first type, referred to in these guidelines as transmission computed tomography (TCT), uses a sealed radioactive source (e.g., Gd-153) with the standard collimated scintillation detectors used for SPECT imaging. The second type of transmission imaging system uses an x-ray tube in conjunction with a computed tomography (CT) detector. The primary differences between these classes of transmission imaging systems include the type of radiation used and the photon emission rate that dictates the quality-control (QC) protocols that are required. The radiation from radioactive source used in TCT is monoenergetic gamma-rays and those used in x-ray CT is polychromatic x-ray from an x-ray tube. Also, the flux of x-ray photons from a typical x-ray tube is much higher than a conventional sealed source used in TCT, CT images can be acquired on the order of seconds to a few minutes depending on the x-ray tube strength.

The number of photons from a sealed radioactive source used to form the transmission image in TCT is on the same magnitude as that from the emission source but much less than that from a typical x-ray tube in CT. As a result, the transmission images obtained from a sealed source has higher noise content than x-ray CT images. Also, scatter photons from the emission source can affect the transmission image obtained from a sealed source but not the x-ray CT images due to the large difference in photon counts. Due to the lower number of photons making up the transmission image and the non-negligible cross-talk scatter component from the injected radiotracer, the TCT QC procedure is slightly more involved and will be outlined separately from the QC for systems using x-ray tubes.

2.7.6. SPECT systems with CT for attenuation correction. Consistent with trends in positron emission tomography (PET)/CT systems, hybrid SPECT/CT systems have evolved, combining SPECT and CT systems. While PET subsystems are generally complete rings or a partial-ring system, the SPECT subsystems are typically large FOV variable-angle dual-

detector systems. These combined systems, in practice, demonstrate a range of capability and integration. The CT subsystems range from non-diagnostic units suitable for use in anatomical localization and attenuation correction to multi-slice (16 slices or more) systems capable of CT angiography and producing diagnostic quality CT images. The SPECT detectors in SPECT/CT systems do not differ in any significant way from those of stand-alone SPECT systems. These systems may be viewed from a protocol perspective as stand-alone systems where an emission study is followed or preceded by a CT scan for attenuation correction. Depending upon the number of CT slices acquired, the CT scanner may be used, as with stand-alone CT scanners, for CT angiography and calcium scoring. The images can then be analyzed independently or in 3D image registration with the SPECT images, depending on the type of study.

2.7.7. System performance. The overall SPECT image quality depends on a combination of the detector performance, collimator dimensions, system design, and image reconstruction algorithm. Whereas conventional SPECT cameras have similar design and performance (depending on the collimator specifications), other systems with nonconventional designs may have much different performance. Laboratories with multiple SPECT systems of different design should ensure that the rest and stress SPECT exams are performed on the same or equivalent scanner.

Basic image quality tests such as spatial resolution, sensitivity, and energy resolution are performed with simple phantoms or procedures. They generally test one or more components of the system performance and, although they provide valuable information, they do not provide a full assessment of the total system performance. Performance assessment is complicated by the fact that resolution and sensitivity vary with respect to the detector orbit, the location in the FOV, and the presence of activity outside the region-of-interest (ROI). Larger fillable phantoms that provide an extended source and a specific imaging test (e.g., hot or cold lesion contrast, uniform volume, myocardial defect detection, etc.) do test the overall imaging procedure and have more value in assessing performance between systems and assuring quality and stability of a specific system.

The image reconstruction algorithm and filter parameters play an important role in the overall image quality. Filtered back projection is standard for conventional SPECT image reconstruction. However, statistical image reconstruction methods with iterative algorithms are now widely used clinically, and some of the newer system designs only support iterative reconstruction algorithms. Many iterative algorithms incorporate modeling of collimator blur and can achieve some degree of resolution recovery. Although reconstructed spatial resolution is often reported from simple phantom tests such as a line source or point source in air, these tests do not provide accurate practical information of system resolution for a specific task (e.g., visualizing a defect in a patient's myocardium).[22] Furthermore, image quality is strongly dependent on the parameters of iterative reconstruction (number of iterations and subsets, regularization parameter, postfilter kernel). For all these reasons, tests with realistic fillable phantoms are essential for performance characterization, and should be included in routine QA.

2.8. QC Procedures

2.8.1. SPECT QC procedures. Appropriate QC procedures (Table 2) are necessary to ensure images of the highest possible technical quality for the equipment used and thus allow the best possible diagnostic service to the patient population.[23] Please note that the frequency of testing requirements may vary from one state to the next, so that it is important to verify that the schedule followed by an individual institution is consistent with that institution's radiation license. For instance, some states require that weekly bar phantoms be performed for all Anger cameras.

Table 2. QC procedures for SPECT systems

Test	Priority	Frequency
Acceptance testing per NEMA	Recommended	Upon delivery, major hardware upgrades
Energy peaking	Mandatory	Daily
Uniformity test	Mandatory	Daily
Resolution and linearity	Recommended	Manufacturer's recommendation
Sensitivity	Optional	Manufacturer's recommendation
Center-of-rotation	Mandatory	Manufacturer's recommendation
Multidetector registration		
Uniformity calibration	Mandatory	Manufacturer's recommendation
Total performance	Recommended	Quarterly

This section outlines the protocols and test frequency for Anger cameras. The manufacturers for cameras based on non-Anger technology should provide comparable protocols for their systems to ensure the optimal operation of their systems for clinical use. If the manufacturer does not provide an equivalent test and the frequency to the tests outlined in this section, the existing guideline protocols and frequencies should be enforced. For manufacturer protocols and frequencies, the manufacturer should provide data that ensures that the measurement has defined tolerance levels (e.g., uniformity has a defined threshold for acceptance). With respect to frequency, these guidelines suggest the expected frequency. The manufacturer should provide data supporting a frequency that is less frequent than what is proposed in these guidelines.

2.8.1.1. Energy peaking. Energy peaking is performed to verify that the camera is counting photons having the correct energy. This test consists of either manually or automatically placing the correct pulse height analyzer's energy window over the photopeak energy to be used. Care must be taken that the technologist verifies the correct placement of the window and that a radioactive point source is used at a distance away of greater than 5 useful FOV (UFOV) diameters from the uncollimated camera; a sheet source is typically used in front of a collimated camera.[24] In either case, the full UFOV of the camera should be illuminated by the source. Window verification should be done even on automated systems where there are single buttons or computer protocols to select for each energy; even in these automated systems, the energy windows tend to drift. These systems allow for window offsets to correct for these drifts. This peaking test should indicate for each camera head whether the camera's automatic peaking circuitry is working properly, whether the peak appears at the correct energy, and whether the shape of the spectrum is correct. If cost, time, and the equipment permit, an electronic or hardcopy screen capture of the spectra with the superimposed energy window should be taken and stored.

2.8.1.2. Uniformity test. Uniformity testing is performed to verify that the camera's sensitivity response is uniform across the detector's face. Some manufacturers recommend that this test be performed intrinsically (using a point source without collimators) while others recommend that this test be performed extrinsically (with the collimator in place in conjunction with a sheet source, usually of Co-57). Advantages of performing intrinsic floods include the fact that the energy of the gamma rays used for the source are identical to energies used clinically, and that no collimator grid patterns are superimposed on the flood. The advantage of performing extrinsic floods is that they are convenient, especially if only one collimator is ever used in conjunction with the Anger camera; also, extrinsic floods can be performed in smaller rooms, whereas intrinsic floods require sufficient distance from source to uncollimated detector. This test consists of exposing the camera with a uniform source of radioactivity, a process commonly referred to as ''flooding'' the detector. If performed intrinsically, a radioactive point source is positioned at a distance at least five times the crystal's UFOV from the center of the detector. This test is usually performed immediately following peaking of the detector. The point source should consist of a small volume (approximately .5 mL) of fluid and low activity (7-11 MBq). For large rectangular cameras (such that the point should be 7-8 ft away), 20-25 MBq is appropriate. In some cameras, obtaining intrinsic flood fields can be difficult. Some manufacturers provide software to correct for nonuniformities due to the necessity of having a point source closer than 5 UFOV diameters. Because of these difficulties, it may be more practical to perform this test extrinsically using radioactive sheet flood sources. To ensure a true response during acquisition, count rates should be kept between 10 and 25 kcps. For some older systems, a lead ring should be used to shield the outermost tubes from the radiation to prevent edge packing. Flood images that will be inspected visually should be acquired as 256×256 matrices for 3 M counts (5 M for larger rectangular detectors). Digitized flood fields should be stored. Flood images used for calculations of uniformity require two to three times more counts to reduce statistical noise. The recommended number of counts is at least 4,500 counts/cm^2 (e.g., 5.7 M counts for a 400-mm circular detector). The National Electrical Manufacturers Association (NEMA) recommends acquiring a minimum of 10,000 counts for the center (6.4 mm) pixel of the flood image.[24]

The flood images should be examined each day for each detector prior to use to verify that the detectors are properly peaked and that the floods are uniform. In addition, several parameters are quantified from the flood images, which should be computed and the results recorded as part of the usual QA procedures. In the event of power shortages and power outages, the process of peaking and flooding the detectors should be performed again to ensure proper function before resuming patient imaging. Two uniformity parameters are computed—integral uniformity and differential uniformity. If the flood images are acquired in a larger matrix size, the pixel matrix should be reduced to 64×64 by summing or averaging pixels prior to uniformity calculation. Integral uniformity is a global parameter measuring uniformity over an extended area of the detector, expressed as follows:

$$\text{Integral uniformity} = 100\% \times (\text{Max} - \text{Min})/(\text{Max} + \text{Min})$$

Max is the maximum count and Min is the minimum count found in any pixel within the specified area. Differential uniformity is a regional parameter that measures contrast over a small neighborhood. This measurement is performed using all 5 × 5 pixel areas in both the X and Y directions, expressed as follows:

$$\text{Differential uniformity} = 100\% \times (\text{Largest deviation } (\text{Max} - \text{Min}))/(\text{Max} + \text{Min})$$

It should be noted that manufacturers vary as to their recommendations regarding the ability of a particular camera to use a flood field collected at one energy (e.g., 140 keV for Tc-99m) to correct the field of data acquired at a different energy (e.g., 70 keV for Tl-201).[25] For some Anger cameras, it may be essential to acquire flood fields separately for Tl-201, I-123, I-131, and so on. In that case, most users will necessarily perform these corrections intrinsically, not extrinsically. Failure to apply an adequate overall flood-field correction is seen most strikingly as concentric ring artifacts on the uniform section of a SPECT Performance Phantom (see Table 3).[23]

2.8.1.3. Resolution and linearity test. This test is performed to document spatial resolution and its change over time as well as the detector's ability to image straight lines. The test consists of imaging a flood source intrinsically through a spatial resolution test phantom. The flood source should be acquired as described in the Uniformity test section. Most commercially available bar phantoms are suitable for this test. These include the parallel-line-equal-space bar phantoms and orthogonal hole or 4-quadrant phantoms. If the 4-quadrant phantom is used, each time the test is conducted, the phantom should be rotated 90° so that every fifth time the test is done, the pattern position repeats. Bar phantom images should be recorded and stored. These images should be assessed for how straight the lines imaged are and for intrinsic spatial resolution. The change in resolution is assessed by documenting the smallest bars that are discerned. Spatial resolution as measured by the FWHM may be approximated by multiplying 1.7 times the smallest bar size seen.[23]

Table 3. Performance parameters for scintillation (or Anger) cameras

Parameter	Standard	Preferred
Integral uniformity	<5%	<3%
Differential uniformity	<5%	<3%
Intrinsic resolution (FWHM)	<6 mm	<4 mm

Note: These values are specific to Anger camera systems using 3/8″ NaI(Tl) crystal.

For imaging systems not based on the Anger camera technology, the manufacturer should provide a QC procedure to insure that the resolution and linearity stability is maintained by the system. In the absence of a manufacturer suggested protocol, this test should be performed at the recommended frequency.

2.8.1.4. Sensitivity test. This test is performed to document the sensitivity of the detector and, more importantly, the change of sensitivity over time. The test consists of calculating detector sensitivity (expressed in terms of counts per minute per megabecquerel) of a known source, calibrated with a dose calibrator. The point source should always be located at exactly the same distance in front of the camera for repeat measurements. A convenient means of measuring sensitivity changes is by recording the time that it takes to acquire the preset counts for an intrinsic (or extrinsic, if more practicable) flood source.

2.8.1.5. Center-of-rotation calibration. An alignment error between the center of the electronic matrix of the camera and the mechanical center-of-rotation (COR) can potentially result in a characteristic ''doughnut'' (if a 360° orbit and a point source are used) or ''tuning fork'' artifact (if a 180° orbit is used) in the transverse images.[26] The effects are most evident when the error is greater than two pixels in a 64 × 64 matrix. Errors less than this reduce spatial resolution and image contrast through blurring of the image and cause significant artifacts (particularly at the apex).[27] The accuracy of COR alignment should be checked weekly for each camera head, unless indicated otherwise by the manufacturer. In some systems, this means that two separate acquisitions are required, one for each detector (with the other detector disabled). Many manufacturers require that a specific protocol be followed for the determination and recalibration of the COR. While some manufacturers limit the COR calibration to service engineers, all systems should be checked for correct COR calibration. If no specific COR acquisition protocol is recommended by the manufacturer, the COR can be determined through the acquisition of a point source of activity (18-37 MBq) on the patient table 4 to 8 inches away from the axis-of-rotation. SPECT data are acquired over 360° with equally spaced projections with a circular orbit. The same angular orientation, collimation, zoom, matrix size, and energy window employed for the patient study should be employed for the COR acquisition. Five to ten seconds per frame for 64 views over 360° is sufficient. COR correction values for each orbit are then computed, stored in the computer, and used to realign the projection data before

Table 4. QC procedures for radionuclide TCT systems

Test	Requirement	Frequency
Energy peaking	Mandatory	Daily*
Transmission source mechanics	Mandatory	Daily*
Source strength	Mandatory	Monthly*

*Or as recommended by the manufacturer.

Table 5. QC Procedures for x-ray CT system

Test	Requirement	Frequency
Calibration	Mandatory	Monthly*
Field uniformity	Mandatory	Monthly*

*Or as recommended by the manufacturer.

Table 6. Schedule of CT QC for SPECT/CT systems

Test	Frequency
Water phantom QA	Daily
Tube warm-up	Daily
Air calibration (''fast QA'')	Daily
Water phantom checks: slice thickness, accuracy, positioning	Monthly

Table 7. Combined SPECT/CT QC procedures

Test	Requirement
Registration	Mandatory
Attenuation correction accuracy	Mandatory

reconstruction. It is essential that COR errors be checked for each collimator that is to be used clinically.[28] It is recommended that these measurements be performed weekly. New COR calibrations should be performed after servicing of the camera, after power surges or outages, and after hardware and software upgrades. It is important to verify that the correct COR information is applied following service of any type, by simply repeating the acquisition of new COR information, and then verifying that a tomographic acquisition of a point source does correctly produce transaxial images that is also a point source.

2.8.1.6. High-count extrinsic flood-field uniformity corrections. Manufacturers vary considerably as to their recommended schedule and means of acquiring these high-count corrections. It has recently been noted that some cameras may not require the acquisition of extrinsic floods more often than annually to verify collimator integrity[12] and that all uniformity corrections should be acquired intrinsically, so long as the camera is correctly tuned.[25] For many systems, collimators are sufficiently well designed and manufactured that they do not degrade SPECT uniformity. Therefore, as with any of the procedures discussed in these guidelines, it is always important to follow the manufacturers' recommended QA protocols. In SPECT, it is implicitly assumed that the efficiency of photon detection is constant across the surface of the collimated detector. Flood-field uniformity errors result when the variation in efficiency is significant as compared to the performance parameters in Table 3. Anger cameras utilize stored flood-field correction maps to correct for variations in sensitivity across the FOV before reconstruction. Deficiencies can lead to characteristic ''ring'' artifacts, most easily seen on the uniform sections of multipurpose Plexiglas SPECT phantoms[23] and myocardial perfusion artifacts. Daily checks of flood-field extrinsic (with collimator) uniformity are performed with a 3-million-count flood for a typical FOV 128 × 128 or 256 × 256 matrix. To correct for sensitivity variations due to the collimator, 30- to 100-million-count images are acquired

Table 8. Minimum accepted criteria for SPECT performance characteristics

Parameter	Accepted range
Reconstructed resolution	Cold rods of diameter greater than or equal to 11.1 mm should be resolved
Reconstructed uniformity	The uniform section of the cylinder should not have ring artifacts in more than one slice. Uniformity within the cylinder should be less than or equal to 20%
Reconstructed contrast	Spheres with diameter 19.1 mm or greater should be clearly visualized. Contrast in the 31.8 mm sphere should be greater than 65%

for each detector (128 × 128 or 256 × 256 matrix) and stored for uniformity correction. It is essential to perform uniformity measurements for each collimator and that the same collimator that was used to acquire the flood and generate the correction matrix be used to acquire the patient study. It is important that energy values similar to those being used for clinical studies also be used for the flood source. Co-57 solid sheet sources (122 keV) are commonly used and, more rarely, fillable sources for Tl-201 and Tc-99m imaging. A solid sheet source is less problematic for daily use. Using the lower-energy correction floods for higher-energy radionuclides can result in incorrect compensation and therefore is not recommended.

2.8.1.7. Multipurpose plexiglas phantoms. It is strongly recommended by NEMA that acquisition and reconstruction of a multipurpose Plexiglas phantom should be performed quarterly at a minimum.[29] For facilities intending to pursue laboratory American College of Radiology (ACR) accreditation, performing these tests is mandatory. In particular, it should be noted that if accreditation is sought from the ACR, it is required to submit acceptable SPECT phantom images for both Tc-99m and Tl-201 simulations. This test should be performed whenever the system has undergone significant servicing or when any of the daily tests exceeds recommended tolerances.

These SPECT phantoms are cylindrical or elliptical water baths into which radioactivity is injected and contain regions with solid spheres of different sizes, regions with solid rods or bars of different sizes alternating with radioactive water, and regions containing only radioactive water.[30] These phantoms are used to determine the 3D contrast, resolution, and uniformity of the scanner, for which high activities (740-925 MBq) and ''fine'' sampling (128 × 128 matrices and 128 projections over 360°) generally are employed.[23] Acquisitions are performed using typical Tc-99m energy settings, with detectors positioned as close to the phantom as is feasible throughout a 360° acquisition, so as to optimize spatial resolution.[1] At least 30 million counts should be acquired, and data then are reconstructed for sections of the phantom to enable assessment of contrast through the center of spheres, 3D resolution through sections of rods, and uniformity through ''blank'' sections. Systemic problems that can be revealed in this fashion include suboptimal energy resolution through failure to display adequate contrast, potential COR problems through loss of resolution through solid rod sections, and inappropriate or inadequate flood-field corrections through the appearance of anomalous concentric rings in uniform sections. These tests should be performed quarterly, as well as following major equipment repairs and installation of new software, to verify the overall ability of the hardware and software to correctly perform tomographic reconstructions.

When used in conjunction with standards established during acceptance testing, these quarterly tests can be helpful in signaling the point at which the manufacturer's service representatives should be called to further diagnose the causes of significant degradation of 3D system performance and to remedy these problems.[25]

2.8.2. Radionuclide TCT QC procedures. QC guidelines need to be followed to ensure that the transmission system using a sealed radioactive source is operating as designed. These tests are tabulated in Table 4.

2.8.2.1. Energy peaking. This test is performed to verify that the camera is counting photons in the proper energy windows. Using a pulse height energy (z) analyzer, which is available on all acquisition stations, the operator should verify that the emission, transmission, and scatter (if applicable) windows are properly set and that photons are being counted in each window. For some systems, this may necessitate manually opening the shutter to the transmission source. If this is not possible, a quick ''blank'' scan (see next paragraph) can be acquired to verify that transmission photons are being properly counted.

2.8.2.2. Transmission source mechanics. When patients are not being imaged, the transmission source is shielded and, on systems where the source translates across the FOV, left in the ''parked'' position. When a patient is imaged, the shutter used to shield the source is opened, allowing transmission photons to be directed toward and through the patient. In some systems, the source will then translate axially along the axis of the body for each projection. To verify the operation of the source shutter and translating mechanics, a reference ''blank'' transmission scan should be acquired. This scan is required for all TCT protocols and is recommended to be acquired weekly and possibly daily prior to the first use of the system for that day. The frequency of this test will depend on the half-life of the isotope of the transmission source and the stability of the TCT system. Follow the manufacturer's recommended acquisition protocol for acquiring a transmission blank scan. When complete, visually inspect planar images and check for artifacts (e.g., focal cold spots, bands of missing data, axial discontinuities). A common misconception is that the blank scan should be uniform, similar to uniformity floods. Stringent uniformity indices of ±10% are not reasonable for the blank scan. Rather, the blank scan should be inspected to ensure that there are no gross non uniformity artifacts (e.g., holes or bands of pixels with no counts). For scanning-source systems, the blank scans should not show discontinuities or abrupt changes in pixel intensity in the axial direction

of the scanning source. The presence of these artifacts is consistent with improper scanning-detection alignment and should be checked by a service engineer.

2.8.2.3. Source strength. For systems using a Gd-153 transmission source, photons collected in the transmission window consist of primary transmission photons and scattered photons (cross-talk) from the emission radiotracer. The ratio of these components, transmission and cross-talk, is referred to as the transmission-to-cross-talk ratio (TCR). This TCR value depends on the transmission source strength, the injected radio-pharmaceutical, the injected activity, and the body habitus. Transmission source decay, higher injected activities, and larger body sizes all tend to decrease the TCR value. Lower TCR values result in reconstructed attenuation maps with increased bias and noise. Since the TCR value will decrease as the source decays, its behavior should be trended over the life of the source, which can guide the user as to when the sources should be replaced. This QC protocol should be performed at least monthly, with the base-line scan being performed when the TCT-ECT system is installed or the transmission sources have been replaced. If the user suspects problems with the TCT-ECT system, a test should be performed immediately prior to using the system for patient imaging. Two protocols are provided, one using a cylinder phantom and the other using an anthropomorphic chest phantom. The chest phantom provides the more comprehensive check of the TCT-ECT system for cardiac imaging compared to the cylinder for obvious reasons. For those sites that may not have access to a chest phantom, the cylinder protocol is provided which is capable of identifying potential problems with a TCT-ECT system.

2.8.3. CT QC procedures. The procedures below should be suitable for ensuring overall proper basic operation of a CT scanner. Table 5 lists recommended CT imaging QC schedules. Some additional procedures may be required by particular manufacturers.

2.8.3.1. Calibration. The reconstructed CT image must exhibit accurate, absolute CT numbers in Hounsfield Units (HU). This is critical for the use of CT images for SPECT attenuation correction, because the quantitative CT values are transformed, usually via a bilinear or trilinear function with one hinge at or near the CT value for water, to the attenuation coefficient for the SPECT radiotracer. Any errors in CT numbers will be propagated as errors in the estimated attenuation coefficients for the radiotracer, which in turn will adversely affect the attenuation-corrected SPECT values. CT system calibration is performed with a special calibration phantom that includes inserts of known CT numbers. This calibration is done by the manufacturer's field service engineers. The CT calibration is then checked daily with a water-filled cylinder, usually 24 cm in diameter provided by the manufacturer. In practice, if the error is greater than 5 HU (i.e., different than the anticipated value of 0 HU), the CT system is considered to be out of calibration. The technologist will usually then do an air calibration, to determine if this corrects the overall calibration (i.e., brings the CT number for water back to within 5 HU of 0). If it does not, the manufacturer's field service engineer must be called. On an annual basis, or after any major repair or calibration, calibration is checked by the manufacturer's service engineer.

2.8.3.2. Field uniformity. The reconstructed CT image must exhibit uniform response throughout the field-of-view (FOV). In practice, this means that a reconstructed image of a uniform water-filled cylinder must itself demonstrate low variation in CT number throughout this image. In practice, small circular regions of interest (ROIs) are placed at the four corners of the cylinder image, and the mean CT number is compared to that from a region in the center of the phantom; the difference in mean region CT number should not exceed 5 HU. Nonuniformities greater than this may produce sufficient quantitative inaccuracies so as to affect SPECT attenuation correction based on the CT image.

Table 6 lists recommended CT QC schedules for combined SPECT/CT Units. Users should consult the manufacturer regarding the specific manner and frequency with which tests should be performed for the CT component of their SPECT/CT device. Both the American College of Radiology (ACR) and American Association of Physicists in Medicine (AAPM) have published CT testing procedural guidelines.[31,32]

2.8.4. Combined transmission (TCT or CT) and SPECT QC procedures. The SPECT and CT portion of the combined system should be assessed as described for the dedicated SPECT and CT imaging devices. In addition to the independent QC tests for the SPECT and CT portions of the combined system, it is necessary to perform additional tests that assess the combined use of SPECT and CT. Table 7 lists recommended QC procedures for combined SPECT/CT units.

2.8.4.1. Registration. The reconstructed SPECT and CT images must accurately reflect the same 3D locations (i.e., the two images must be in registration). Such registration is often difficult because the SPECT and CT portions of all commercial combined SPECT/CT systems are not coincident (i.e., the SPECT and CT ''slices'' are not in the same plane) and because the SPECT and CT gantries are contiguous. In practice, this means that the SPECT and CT acquisitions do not simultaneously image the same slice. In fact, because the bed must travel different distances into the gantry to image the same slice in the patient for SPECT vs CT, there

is ample opportunity for misregistration via *x*, *y*, *z* misalignment of bed motion—or, of perhaps even greater concern, because of differential ''bed sag'' for the SPECT and CT portions, depending on the table design.

In addition, electronic drift can influence the ''position'' of each image, so that calibrations for mechanical registration can become inaccurate over time. Thus, it is imperative to check SPECT-to-CT registration on an ongoing basis. This is usually performed with a specific phantom or jig containing an array of point sources visible in both SPECT and CT.

Errors in co-location in the fused SPECT-CT images are assessed, such as by means of count profiles generated across transaxial slices. Such errors, after software registration corrections, should be <1 mm. It is important to image this registration jig in a number of positions along the bed. It may also be helpful to place a weight on the end of the bed to produce some bed sag and repeat the assessment.

Note: The above considerations are in addition to the patient-specific alignment QC clinically necessary to assess possible patient or respiratory motion (not described here).

2.8.4.2. Attenuation correction accuracy. The use of the CT image for SPECT attenuation correction requires a transformation of the CT attenuation coefficients to the attenuation coefficients for the SPECT radiotracer. This transformation is usually accomplished with a bilinear or trilinear calibration curve, with one ''hinge'' at the attenuation coefficient for water.

At a minimum, it is important to image a water-filled cylinder to assess SPECT field uniformity and SPECT activity concentrations after CT-based SPECT attenuation correction. Errors in CT-to-SPECT attenuation transformations are usually manifest as a corrected SPECT image without a ''flat'' profile from edge to center (i.e., the activity at the edge is either too high or too low relative to that at the center of the phantom) and with resulting attenuation-corrected absolute SPECT values that are incorrect (although these values depend on absolute SPECT scanner calibration as well as accurate CT-based SPECT attenuation correction).

2.8.5. Camera acceptance. It is recommended that the NEMA performance measurements (NU 1-2007)[24] be made before accepting the SPECT scanner.[25] Many of these tests can be performed by the company supplying the SPECT scanner. If so, it is recommended that the purchaser's representative work with the manufacturer's representatives during these tests, as the manufacturer may not perform them as specified by NEMA recommendations.

For new technologies that may not yet be addressed by the NEMA specifications,[33] the following imaging guideline is intended to provide an appropriate means of assessing new equipment function in conjunction with nuclear cardiology imaging. Because imaging systems can vary considerably with the optimal manner in which to perform specific tests, this document should be used as a guideline only and is not intended to replace the recommendations by manufacturers of specific models of imaging equipment. Using an approved multipurpose Plexiglas phantom that can be imaged within the sampled field of view of the system, the standard minimum acceptable values for SPECT image acquisition and processing for new technology are defined in Table 8. These values are intended to define an output of image quality that would be comparable to existing SPECT image quality acquired and processed using a collimated scintillation camera.

3. ACQUISITION PROTOCOLS

Protocols for the various nuclear cardiology SPECT acquisition studies using Anger camera technology and conventional filtered backprojection reconstruction are presented in Tables 12-17. For each of the protocols the acquisition parameters and values are listed for the stress and rest portions of the protocol. A description for each of the acquisition parameters is listed below.

Implementation of these protocol acquisition parameters have been shown to provide acceptable images of good quality for routine clinical interpretation and quantitation. These protocols should be viewed as a consensus of opinion on the parameters that will provide acceptable images. However, protocol parameters that reduce imaging time and/or require reduced doses of radiopharmaceuticals other than those listed below have been recently validated in smaller, single center studies and thus may be preferred at some institutions. These studies involve the application of algorithms for, attenuation correction, scatter correction, resolution recovery, collimator-specific geometric response characteristics, and camera response depth-dependence that result in similar or superior image quality to the accepted parameters outlined below. A description for each of the acquisition parameters is listed below.

In addition, stress-only imaging has been used as a means to reduce the radiation dose to the patient and reduce the time spent in the lab. With this protocol, if the stress images are normal, rest imaging is not necessary. Patients with normal stress-only images (with attenuation correction) have been shown to have similar outcomes to those with normal stress-rest images.[34] Isotope dosing in these studies depends on whether the study will be completed in one day or two days if the stress study is not clearly normal. If the plan is for a one day study, then a relatively low dose (8-15 mCi) of a technetium agent is used for the stress study. If a two-

day study will be necessary (such as with larger patients), a high dose (30 mCi) of a technetium agent is used. The reader is referred to Tables 13 and 14 for descriptions of the appropriate stress acquisition parameters for one and two-day technetium protocols.

There are several new technologies, both hardware and software, that are not covered by these tables due to multiple factors (e.g., vendor specific technologies, insufficient clinical data). For these ''newer'' technologies, the reader is advised to consult the manufacturer's recommended protocols and the supporting data for the use of the clinical use of these protocols. Regardless of instrumentation, acquisition or processing protocols, there are several parameters that are common and need explanation.

3.1. Dose

The standard doses described are given for an average 70-kg patient. Doses may be adjusted upward for heavier patients by .04 mCi/kg for Tl-201 and by .31 mCi/kg for Tc-99m. Dose reduction techniques can be employed by increasing the acquisition time. For newer technologies, both hardware and software, the standard doses may be adjusted based on the vendor recommended protocol.

3.2. Position

Factors influencing patient position include camera/gantry design, minimization of artifacts, and patient comfort. Supine position is routinely used for SPECT imaging with most currently available systems and protocols. Prone imaging has been reported to produce less patient motion and less inferior wall attenuation than supine imaging.[35,36] The combination of supine and prone images may be helpful in identifying attenuation artifacts due to breast and/or excessive lateral chest-wall fat, due to the shift in position of the attenuating structures that occur in the prone position. In some laboratories, the advantages of prone imaging in clarifying artifactual defects has lead to a routine use of the combination of supine followed by prone acquisitions.[37] It appears that prone imaging does not eliminate attenuation artifact but rather simply changes the location. By comparing supine and prone images, artifactual defects will change their location whereas true perfusion defects will remain fixed.[38,39] When being used in this fashion, the acquisition time for the secondary (prone) image set is reduced by 20-40%. Some camera/gantry designs require the patient to be positioned in a more upright position. Changes in patient positioning from those described above will likely cause changes in the distribution of adjacent soft tissue attenuation and need to be considered in image interpretation. New normal databases will most likely need to be generated for different patient positions.

3.3. Delay Time

These times are listed as ranges; specific values are optional. The objectives are to allow the patient to recover fully from exercise thus allowing heart rate to return to baseline (reducing gating artifact), avoiding ''upward creep'' from changes in respiratory patterns while dyspnea resolves and to minimize interference from hepatic uptake.[40] Provided that imaging times fall within the specified ranges, clinically useful SPECT images should result. With Tl-201, imaging should be begun approximately 10-15 minutes after stress testing, and if soft tissue attenuation or patient motion compromises a study, the benefit of repeating the acquisition is questionable. In contrast, Tc-99m sestamibi or Tc-99m tetrofosmin allow delayed imaged and therefore permit stress testing and tracer injection to take place at a location remote from the imaging laboratory and image acquisition can simply be repeated when patient motion, soft tissue attenuation or other artifact is considered to be responsible for the production of a perfusion defect.

3.4. Energy Windows

Energy window position is determined by the radioisotope employed, 140 keV for technetium-based perfusion agents and 70 keV for thallium. It is reasonable to simultaneously acquire the higher energy peaks of thallium (135 and 167 keV) on cameras that are capable of doing this. The window sizes are determined largely by the imaging systems (i.e., detector material) and most often reflect the tradeoff between image counts and resolution. For the tables in the Appendices, the values are the most commonly used for Anger cameras using NaI(Tl) crystals. On systems offering improved energy resolution (solid-state detector and crystals), the window size may be reduced, resulting in decreased scatter and improved image resolution. The same energy windows used in performing patient studies should be used for routine daily quality control.

3.5. Collimator

For conventional Anger imaging systems, parallel-hole collimators are most commonly employed for cardiac SPECT acquisitions. They fall into two categories: low-energy all-purpose (LEAP), used mostly for Tl-201 studies, and low-energy high-resolution (LEHR), used for Tc-99m studies. Compared with LEAP collimators,

LEHR collimators have longer bores, thinner septa, and smaller holes, which provide better resolution at the expense of reduced sensitivity. Therefore, to use LEHR collimators, imaging agents providing high-count rates are required (i.e., Tc-99m agents). Generally, LEAP collimators are used for 3-mCi Tl-201 studies, including gated SPECT acquisitions. For protocols using Tc-99m labeled tracers, LEHR collimators are preferred. The collimator is the main factor that limits count sensitivity of Anger cameras. Some of the newer detector designs have been reported to provide 3-5 times the count sensitivity of conventional Anger camera tomography.[1] Emerging camera technologies are employing novel collimator designs to increase imaging sensitivity of the heart.

3.6. Angular Sampling Range

Because of the anterior position of the heart in the left hemithorax, the preferred orbit or angular sample range is 180° from 45° RAO to 45° LPO. The utility of the posterior 180° of a 360° orbit is much greater for higher-energy radioisotopes (such as technetium) compared to low-energy radioisotopes (such as thallium). The recommended orbit range is largely dependent on the camera configuration and the choice should consider the manufacturer's recommendation.

3.7. Number of Projections

The optimal number of projections for emission studies depends on matching the number of projections to the resolution of the system. A thallium SPECT acquisition with a LEAP collimator is a relatively low-resolution study, for which 32 projections over 180° are sufficient. A higher-resolution study using Tc-99m agents should be collected with a high-resolution collimator; this requires at least 60-64 projections over 180° to prevent loss of resolution. For nonrotating Anger system, the number of projections is dependent on the imaging system and the choice should consider the manufacturer's recommendation.

3.8. Orbit Type

For rotating detector systems, the main orbit options for SPECT cardiac imaging are circular and noncircular (elliptical or body-contoured) orbits. Noncircular orbits follow the contour of the patient, bringing the camera closer to the patient, thereby improving spatial resolution. Circular orbits maintain a fixed radius of rotation and on average result in the detector being further from the patient. In general, there is reduced (but more uniform) spatial resolution with circular orbits since the detector-to-source distance is greater with this technique. Manufacturers are more commonly providing excellent noncircular orbit capability with the ability to minify the negative impact of variation of source-to-detector distance.

3.9. Pixel Size

For current cardiac SPECT imaging systems, the imaging resolution is between 13 and 16 mm. For spatial sampling, it is desired to have two to three pixels over the imaging resolution which provides a usable pixel range of 4.5-7.0 mm per pixel. Tables 12-17 specify a 6.4 ± .4 mm pixel size for a 64 × 64 image matrix which has been extensively used with current Anger technology. This size offers satisfactory image resolution for interpretation and quantitation of both Tl-201 and Tc-99m tomograms.

3.10. Acquisition Type

The most widespread mode of tomographic acquisition is the ''step-and-shoot'' method. In this approach, the camera acquires a projection then stops recording data when moving to the next angle; this results in a small amount of dead time since the camera is not acquiring data while it is moving. An alternative is ''continuous'' mode where the camera moves continuously and acquires each projection over an angular increment. This eliminates dead time and thus increases image counts at the expense of a small amount of blurring due to the motion of the camera head while acquiring. It seems likely that the increase in count statistics more than offsets the small amount of blurring due to camera motion. Other systems without rotating heads are described above.

3.11. Matrix

The standard matrix size for Anger cameras is 64 × 64 or 128 × 128 pixels, depending on the field of view and zoom factor. Users should refer to manufacturer's recommendations for specific scanners and configurations.

3.12. Acquisition Time

The total time for an emission acquisition ultimately is based on how long a patient can tolerate the procedure without moving, balanced by the need to acquire sufficient counts. The maximum practical time is on the order of 20 minutes. The acquisition times provided in the tables in the Appendices have been found to produce images of acceptable and comparable quality for rest

and stress studies. These times may not be optimal for systems with greater sensitivity (e.g., multidetector, half ring) and should be adjusted based on the manufacturer's recommendation and validation of its use.

3.13. Gating

The introduction of technetium-based perfusion tracers has resulted in images with sufficient count density to allow for cardiac gating adding parameters of wall motion, wall thickening, and EF to myocardial perfusion imaging.[41-44] Gating requires a stable and consistent heart rhythm as well as sufficient temporal resolution to correctly characterize the cardiac cycle. A stable heart rate and rhythm can be achieved by rejecting heartbeats that fall out of range at the expense of an increase in image time. This ''beat length acceptance window'' can vary from 20% to 100% of the expected R-to-R duration; the recommended value being 20% if an ''extra frame'' is provided that allows the accumulation of rejected counts. Most laboratories gate the heart for eight frames per cycle, although an increasing number of laboratories have reported good results with 16 frames per cycle and have used the increased temporal sampling to derive more accurate estimates of LVEF as well as parameters of diastolic function. For either 8- or 16-frame gating, the recommendations are to avoid beat rejection. The lower count statistics achieved with Tl-201 imaging makes gating more challenging with this isotope, but many laboratories have reported satisfactory results using 8-frame gating in selected patients.[45] Providing that there is adequate count density, particularly with regard to the lower dose acquisitions, it is recommended that both stress and rest SPECT perfusion studies be acquired as gated data sets.

4. PROCESSING PROTOCOLS

4.1. Filtering

Image filtering is a very complex topic that encompasses techniques for image enhancement, reconstruction, and feature extraction.[46,47] The main area of concern for an interpreter of SPECT studies is image enhancement via noise reduction. All forms of imaging are plagued by statistical variation in the acquired image counts commonly referred to as noise. The quality of an image can be described the signal-to-noise ratio, which describes the relative strength of the signal component (what is actually being imaged) compared to noise. The signal to-noise-ratio is much higher at lower spatial frequencies (broad features that are constant over many pixels) and decreases at higher spatial frequencies (features that change over few pixels such as edges). In general, the greater the count statistics, the better the signal-to-noise ratio. A low-pass filter is generally used to reduce noise because it allows low spatial frequencies to pass through and attenuates the high frequencies where image noise predominates. Low-pass filters such as the Hanning and Butterworth can be characterized by a cut-off frequency where they begin to affect the image. The cut-off frequency can be adjusted, depending on the signal-to-noise ratio to preserve as much of the signal and suppress[48] as much noise as possible. If the cut-off is too high, there is significant noise in the image; if the cut-off is too low, significant information in the signal is suppressed. Nuclear cardiology images, because of their relatively low count statistics, tend to have greater amounts of image noise and filtered back projection, because of its dependence on ramp filtering, tends to amplify this noise. The optimal filter for a given image depends on the signal-to-noise ratio for that image; under-filtering an image leaves significant noise in the image, and over-filtering unnecessarily blurs image detail; both over-filtering and under-filtering can reduce image accuracy. Software reconstruction packages are set with default filter selection and cut-off values that are optimized for the average patient. Adjustment of the filter cut-off can be done in patients with poor count statistics (e.g., obese patients) to optimally filter their images. However, this is discouraged unless the physician is thoroughly familiar with filter adjustment and the potential effects. Changing the filter cutoff may have unexpected effects on the output of commercially available analysis programs, especially those that employ edge detection such as defect quantitation and LV volumes and EF. Deconvolving filters, such as the Metz and Wiener filters can correct for blurring that occurs from scatter as photons travel through the body. Although images may look sharper with these filters, these filters have not yet been shown to improve image accuracy.[46]

4.2. Reconstruction

4.2.1. Filtered backprojection. The traditional method of image reconstruction has been filtered backprojection, a technique based on a mathematical proof, which assumes perfect line integral count profiles (i.e., perfect collimation), no attenuation, no scatter, and an infinite number of projections. It is relatively straightforward and comparatively fast.[49] The vast majority of clinical experience is based upon it and it has withstood the test of time despite its inability to model real world collimation, attenuation and scatter. Simple backprojection of acquired count profiles (a single row of pixels from each projection) results in an image which appears blurred by a function of $1/r$ where 'r' equals the

radial distance in the Fourier domain. To suppress this blurring, each profile is filtered in the Fourier domain with the ramp filter prior to back projection (filtered backprojection). As noted above, application of the ramp filter, although suppressing low frequency $1/r$ blurring, amplifies the already relatively noisy high-frequency content of the acquired profiles. Therefore, it is a combination of the ramp filter and a low pass, noise suppression filter (e.g., Butterworth) that is ultimately used to filter the projection data prior to back projection.

4.2.2. Iterative reconstruction. There is a different class of reconstruction algorithms that is based on iterative techniques. These algorithms start with a rudimentary guess of the distribution, generate projections from the guess, and compare these projections to the acquired projections. The guess is refined based on the differences between the generated and actual projections and the process is repeated (hence the term ''iterative'') usually for a fixed number of iterations but can also be repeated until the error between the generated and actual projections is acceptably small. A main advantage of these algorithms is that the process of generating projections from the guess can be made as sophisticated as desired and can incorporate corrections for attenuation, scatter, and collimator specific, depth-dependent blurring. Various iterative algorithms have been developed including, but not limited to, expectation maximization (EM), MLEM, and maximum a posteriori (MAP) techniques. The primary differences between these algorithms are the methods by which reprojected data (the guess) is compared and updated relative to the acquired projections and differences in noise modeling and compensation. A disadvantage of iterative reconstruction is the computational intensity of the algorithms; it takes many times longer to complete than filtered back projection. In an effort to decrease reconstruction time, the OSEM algorithm was developed. This technique uses a subset of the acquired projection data during each iteration with the number of subsets speeding the reconstruction time by roughly the same factor—i.e., a reconstruction using four iterations with eight subsets completes roughly eight times faster than a non-subsetted EM reconstruction.[50] This technique, coupled with the continual increase in computing power, allow iterative reconstructions to be completed in an acceptable time for routine clinical use. Nonetheless, iterative techniques have not yet been proven to be unequivocally superior to filtered back projection. The reconstruction methods discussed thus far generally reconstruct, in isolation, one transaxial two-dimensional (2D) slice per projection count profile—one row of pixels from each projection reconstructs and creates a single slice, each derived independently from the previous or next. Newly available iterative techniques use data from adjacent count profiles and 2D slices to better model data acquisition and 3D tracer distribution. For example, instead of modeling collimator point spread functions simply in the 2D transaxial plane (fan beam), collimator depth-dependent de-blurring can be applied incorporating data in the axial direction as well (cone beam), across multiple 2D slices—i.e., 3D reconstruction. Most use an OSEM algorithm that can be broadly characterized as a 3D-OSEM technique. These techniques can compensate for the increased noise of low count acquisitions, thus allowing for a decrease in scan times (half time or quarter time imaging has been investigated)[51-53] or a reduction in injected dose and therefore decreased patient radiation exposure.

4.3. Reorientation

A critical phase of myocardial processing is reorientation of tomographic data into the natural approximate symmetry axes of an individual patient's heart. This is performed either manually or automatically and results in sectioning the data into vertical long-axis, horizontal long-axis, and short-axis planes. Long-axis orientation lines should be parallel to long-axis walls of the myocardium and should be consistent between rest and stress studies. Inappropriate plane selections can result in misaligned myocardial walls between rest and stress data sets, potentially resulting in incorrect interpretation. It is crucial that all axis choices be available as QC screens, and that these are reviewed by the technologist and the physician who reads each study to verify that axes were selected properly.

4.4. Display

4.4.1. Cine review. The most important post-acquisition QC procedure is to view the raw tomographic data in cine mode. This presentation offers a sensitive method for detecting patient and/or heart motion, ''upward creep,'' breast shadow due to attenuation, diaphragmatic attenuation, and superimposed abdominal visceral activity, all of which can create artifacts in the reconstructed images. Review of the raw tomograms in cine mode is performed twice: once by the technologist immediately after the acquisition, and again by the physician during image interpretation. For gated studies, usually it is only the sum of all gated tomograms that is reviewed in this manor; but cine review of all tomographic data (i.e., projections through all phases of the cardiac cycle) may alert the observer to gating errors due to arrhythmias manifested by as intermittent flashing of the images. A full display of all count-vs-projection curve data may be helpful. Display and review of the beat histogram (relative number of beats collected at

specific R-R intervals) may also assist in determining if a observed abnormal cardiac wall motion is real or artifactual. Cine reviews occasionally show abnormalities in the abdomen or thorax such as renal cysts or abnormal uptake that may be suspicious for neoplasm. The accuracy and clinical utility of these findings has not yet been established.

4.4.2. Study review. It is strongly recommended that physicians use a computer display for reviewing images and use film and paper hard copies, if at all, only for record-keeping purposes. Images produced by formatters onto transparency film or photographic paper can have variable contrast, also termed gamma, and result in inconsistent image interpretation. Computer screen outputs are relatively more stable, and always have readily available monochromatic contrast bars or color code bars to the side of the images, enabling more consistent viewing conditions. In addition, computer screens offer rapid sequential and/or cinematic displays of image data. For all of these reasons, screen interpretation is strongly recommended over relying on interpretations from hard copies.[54]

5. INTERPRETATION AND REPORTING

5.1. General Comments

The interpretation of myocardial perfusion SPECT images should be performed in a systematic fashion to include: (1) evaluation of the raw images in cine mode to determine the presence of potential sources of image artifact and the distribution of extracardiac tracer activity; (2) interpretation of images with respect to the location, size, severity, and reversibility of perfusion defects as well as cardiac chamber sizes, and, especially for Tl-201, presence or absence of increased pulmonary uptake; (3) incorporation of the results of quantitative perfusion analysis; (4) consideration of functional data obtained from the gated images; and (5) consideration of clinical factors that may influence the final interpretation of the study. All of these factors contribute to the production of a final clinical report. Guidelines for interpretation and reporting of myocardial perfusion SPECT are listed in Tables 9 and 10.

5.2. Display

5.2.1. Recommended medium for display. It is strongly recommended that the reading physician use the computer monitor screen rather than hard copy (e.g., paper or film) to interpret the study. A computer monitor is capable of displaying more

Table 9. Myocardial perfusion SPECT: guidelines for interpretation

Display	
Medium	
Computer screen	Preferred
Film hard copy	Discouraged
Format	
Conventional slice display	Preferred
Frame normalization	Optional
Series normalization	Preferred
Three-dimensional display	Optional
Technical sources of error	
Motion	Standard
Attenuation	Standard
Attenuation correction	Optional
Reconstruction artifacts	Standard
Myocardial statistics	Standard
Initial image interpretation	
Ventricular dilation	
Qualitative	Standard
Quantitative	Optional
Lung uptake	
Qualitative	Standard
Quantitative	Preferred
Noncardiac	Standard
Perfusion defect assessment	
Location	Standard
Extent/severity	
Qualitative	Standard
Semiquantitative	Optional
Quantitative	Optional
Reversibility	Standard
Gated SPECT	
Display	Standard
Quality control	Standard
Regional wall motion	Standard
Regional wall thickening	Standard
LV ejection fraction	
Qualitative	Standard
Quantitative	Preferred
LV volume	
Qualitative	Standard
Quantitative	Recommended
Integration of perfusion and function results	Standard
Myocardial viability	
Qualitative	Standard
Semiquantitative	Optional
Quantitative	Preferred
Modification of interpretation	Preferred

Table 10. Myocardial perfusion SPECT: guideline for reporting

Demographic and study referral data	
Name	Required
Gender	Required
Age	Required
Date(s) of acquisition(s)	Required
Medical record identification	Required
Height/weight (body surface area)	Recommended
Relevant medications	Recommended
Indication for study	Required
Referring clinician	Required
Interpreting physician	Required
Acquisition parameters	
Type(s) of studies	Required
Radionuclide(s) and doses	Required
Patient position (supine, prone, upright)	Recommended
Use of gating and/or attenuation correction	Required
Results: stress data	
Resting ECG findings	Required
Stress parameters	
Heart rate, blood pressure, % maximal predicted heart rate, metabolic equivalents	Required
Symptoms	Required
Reason for termination	Required
ECG changes with stress	Required
Results: perfusion data	
Quality	Required
Potential sources of error	Required
Lung uptake (thallium)	Optional
Perfusion defect	
Location	Required
Extent as % of myocardium	Recommended
Defect severity	Required
Type of defect (ischemic, scar, mixed)	Required
TCD/TID	Required
TCD/TID quantitative	Optional
RV activity	Recommended
Results: gated SPECT	
Regional wall motion, thickening	Recommended
Global function	
Qualitative	Required
Quantitative	Required
LV volume	Optional
Overall study quality	Required
Conclusion	
Normal/abnormal/equivocal	Required
Artifact(s)	Recommended
Abnormal noncardiac uptake	Recommended
Comparison to prior studies	Recommended
Probability of CAD	Optional
Date of interpretation	Required
Signature	Required

variations in gray scale or color, making it easier to discern smaller variations in activity. Moreover, it is not possible to properly view moving images (e.g., raw cine data or gated images) on hard copy. A linear gray-scale translation table is generally preferred to color tables since the gray-scale demonstrates more consistent grades of uptake, but this is also dependent on the familiarity of the individual reader with a given translation table.[54,55] The reader should be aware that the appearance of an image can change significantly when changing from one translation table to another. A linear scale is preferred to nonlinear (e.g., sigmoidal) scales since it most faithfully characterizes uptake over the range of activity. A logarithmic scale may be used for evaluating regions of lower count density such as soft tissue uptake and the right ventricle (RV) but should never be used for interpreting regional LV uptake.[54]

5.2.2. Conventional slice display of SPECT images. Three sets of tomographic images should be displayed: (1) a view generated by slicing perpendicular to the long-axis of the LV (short-axis); (2) a view of long-axis tomograms generated by slicing in the vertical plane (vertical long-axis); and (3) a view of long-axis tomograms generated by slicing in the horizontal plane (horizontal long-axis). The short-axis tomograms should be displayed with the apical slices to the left and the base at the right. The vertical long-axis tomograms should be displayed with septal slices on the left and the lateral slices on the right. Similarly, the horizontal long-axis tomograms should be displayed with inferior slices on the left and anterior slices on the right. It is also recommended that, for purposes of comparison of sequential images (e.g., stress and rest, rest and redistribution), the sequential images should be displayed aligned and adjacent to each other.

There are two widely used approaches to image normalization. Each series (vertical, horizontal, short-axis) may be normalized to the brightest pixel in the entire image set, which is known as ''series normalization.'' This is considered to provide the most intuitively easy way to evaluate the extent and severity of perfusion defects. The drawbacks of this approach are its sensitivity to focal hot spots, the frequently poor visualization of normal structures at the base and apex of the LV, and the lack of an ideal display of each individual slice. The

other approach is ''frame normalization'' in which each frame (slice) is normalized to the brightest pixel within the frame (slice). This method provides optimal image quality for each slice. The drawback of this approach is that the brightness of each slice is unrelated to the peak myocardial activity in the entire series such that gradations in activity between slices of a series may not be appreciated; however, it is mitigated by the display of three orthogonal planes.

5.2.3. Three-dimensional display. Most commercial software programs allow creation of 3D displays of regional myocardial perfusion. These displays may help less experienced readers identify coronary distributions associated with perfusion defects, but 3D displays should be used only as an adjunct to, not a replacement for, the conventional image formatting described above.

5.3. Evaluation of the Images for Technical Sources of Error

5.3.1. Patient motion. The interpreting physician should review the raw planar images for possible sources of attenuation artifact and for the presence of patient motion. A cine display of the planar projection data is highly recommended because motion in both the vertical (craniocaudal) and horizontal (side-to-side) axes are readily detectable. Additionally, a static ''sinogram'' or ''linogram'' may be used to detect patient motion. Software programs are available for the quantitation and correction of patient motion. The experienced reader should be familiar with the normal appearance of raw planar images and be able to identify motion artifact. In patients who have had a technetium-based perfusion agent with negligible myocardial redistribution (e.g., Tc-99m sestamibi or Tc-99m tetrofosmin), consideration should be made for repeating the image acquisition when significant motion is detected. Alternatives, such as planar imaging or prone positioning may also be considered. The effect of patient motion on the final reconstructions is complex.[56,57] Generally, vertical (i.e., craniocaudal) motion has less of an effect on the accuracy of the study than horizontal (side-to-side) motion, especially when the heart returns to the same baseline. Vertical motion is also much easier to correct manually or with semi-automated software. Rotation currently cannot be corrected either manually or with available motion correction software. Since motion correction software may sometimes introduce motion artifact, corrected raw planar images should be evaluated for adequacy of the correction.

5.3.2. Attenuation and attenuation correction. The cine display of the planar projection images is also recommended for the identification of sources of attenuation, the most common being diaphragmatic in men and the breast in women.[58] Breast attenuation artifact is most problematic when the left breast position varies between the rest and stress images (i.e., ''shifting breast attenuation artifact''). When the apparent perfusion defect caused by breast attenuation artifact is more severe on the stress images than on the resting images, it is difficult to exclude ischemia. Breast attenuation artifact can be confirmed by repeating the acquisition with the left breast repositioned. Diaphragmatic attenuation and breast attenuation may also be addressed by imaging the patient prone. Hardware and software for attenuation and scatter correction are commercially available and may obviate or at least mitigate these common attenuation artifacts. The evaluation of attenuation-corrected images is performed with the same approach as that used for non-attenuation-corrected images. As with the interpretation of non-attenuation-corrected studies, it is essential that the interpreting physician be familiar with the segment-by-segment normal variation of uptake of radioactivity at stress and rest associated with the specific attenuation correction system that is being used.[59-61] Attenuation-corrected images are displayed in the same manner as uncorrected images. Because the currently available correction algorithms are imperfect, it is recommended that the uncorrected data be interpreted along with the attenuation-corrected data.

5.3.3. Reconstruction artifacts. Intense extracardiac tracer activity in very close proximity to the heart (e.g., superimposed bowel loops or liver activity) may create artifactually increased uptake in adjacent myocardium that could mask a perfusion defect or be misinterpreted as reduced uptake in remote myocardial segments. Nonsuperimposed but adjacent extracardiac activity may also cause a negative reconstruction artifact, resulting in an apparent reduction in activity in the adjacent myocardial segment. There is currently no reliable correction for such artifacts, although they may be less problematic with iterative as opposed to filtered back projection reconstruction techniques. These artifacts can often be eliminated by repeating the acquisition after the activity level in the adjacent extracardiac structure has decreased.

5.3.4. Myocardial statistics. Many factors are involved in the final count density of perfusion images including body habitus, exercise level achieved, radiopharmaceutical dose, acquisition time, energy window, and collimation. Apparent perfusion defects can be artifactually created simply because of low image count density. The interpreting physician should make note of the count density in the planar projection images because the quality of the reconstructed data is a direct reflection of the count rates measured on the raw data. As a general rule, peak pixel activity in the LV

myocardium in an anterior planar projection should exceed 100 counts for a Tl-201 study and 200 counts in a Tc-99m study.

5.4. Initial Image Analysis and Interpretation

The initial interpretation of the perfusion study should be performed without any clinical information other than the patient's gender, height and weight. Such an approach minimizes the bias in study interpretation. All relevant clinical data should be reviewed after a preliminary impression is formed.

5.4.1. Ventricular dilation. Before segmental analysis of myocardial perfusion, the reader should note whether or not there is LV enlargement at rest or post-stress. Dilation of the LV on both the stress and resting studies usually indicates LV systolic dysfunction, although it may be seen in volume overload states (e.g., severe mitral or aortic regurgitation) with normal ventricular systolic function. An increased stress-to-rest LV cavity ratio, also referred to as transient cavity dilatation (TCD) or transient ischemic dilation (TID), has been described as a marker for high-risk coronary disease.[62,63] It is actually apparent, and not true, dilatation of the ventricle with stress, and is most likely caused by diffuse subendocardial ischemia[64,65] and can be seen in other conditions, such as microvascular disease, that cause diffuse subendocardial ischemia even in the absence of epicardial coronary disease. TID is typically described qualitatively but may also be quantified.[66,67] Normal limits by quantitation will depend on perfusion imaging protocol, the image processing parameters, and the software algorithm used.

5.4.2. Lung uptake. The presence of increased lung uptake after thallium perfusion imaging has been described as an indicator of poor prognosis and should therefore be evaluated in all patients when using this perfusion agent.[64,65,68] No clear consensus has emerged as to the significance of lung uptake with technetium-based perfusion agents, although increased lung Tc-99m tracer uptake may provide a clue to the presence of resting LV systolic dysfunction in patients who are not candidates for gated SPECT imaging due to severe arrhythmias.

5.4.3. Right ventricular uptake. Right ventricular RV uptake may be qualitatively assessed on the raw projection data and on the reconstructed data. There are no established quantitative criteria for RV uptake, but in general, the intensity of the RV is approximately 50% of peak LV intensity. RV uptake increases in the presence of RV hypertrophy, most typically because of pulmonary hypertension.[69] The intensity of the RV may also appear relatively increased when LV uptake is globally reduced.[70] Regional abnormalities of RV uptake may be a sign of ischemia or infarction in the distribution of the right coronary artery. The size of the RV should also be noted, as RV dilation can provide a clue to the presence of right heart volume overload due to conditions such as atrial septal defect or severe tricuspid regurgitation.

5.4.4. Noncardiac findings. Both thallium- and technetium-based agents can be concentrated in tumors, and uptake outside the myocardium may reflect unexpected pathology.[71] However, the sensitivity and specificity of myocardial perfusion imaging for diagnosing noncardiac conditions have not been well established. Splanchnic tracer activity following adequate exercise stress (i.e., greater than 85% maximum predicted heart rate) is generally reduced compared to resting images. This difference is not present following pharmacologic stress testing with dipyridamole, adenosine, regadenoson, or dobutamine.

5.4.5. Perfusion defect location. Myocardial perfusion defects should be identified by the use of visual analysis of the reconstructed slices. The perfusion defects should be characterized by their location as they relate to specific myocardial walls—that is, apical, anterior, inferior, and lateral. The term posterior should be avoided because it has been variably assigned to either the lateral wall (circumflex distribution) or to the basal inferior wall (right coronary distribution), and is thus ambiguous. Standardization of segment nomenclature is highly recommended[72] (see the segmentation models depicted in Fig. 1 and Table 11).

5.4.6. Perfusion defect severity and extent.

5.4.6.1. Qualitative. Defect severity is typically expressed qualitatively as mild, moderate, or severe. Mild defects may be identified by a decrease in counts

SPECT Myocardial Perfusion Imaging	
1. basal anterior	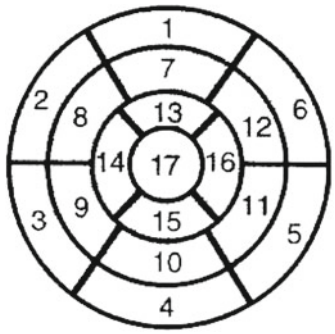
2. basal anteroseptal	
3. basal inferoseptal	
4. basal inferior	
5. basal inferolateral	
6. basal anterolateral	
7. mid anterior	
8. mid anteroseptal	
9. mid inferoseptal	
10. mid inferior	
11. mid inferolateral	
12. mid anterolateral	
13. apical anterior	
14. apical septal	
15. apical inferior	
16. apical lateral	
17. apex	

Figure 1. SPECT myocardial perfusion imaging: 17-segment model.

Table 11. The five-point model

Category	Score
Normal perfusion	0
Mild reduction in counts—not definitely abnormal	1
Moderate reduction in counts—definitely abnormal	2
Severe reduction in counts	3
Absent uptake	4

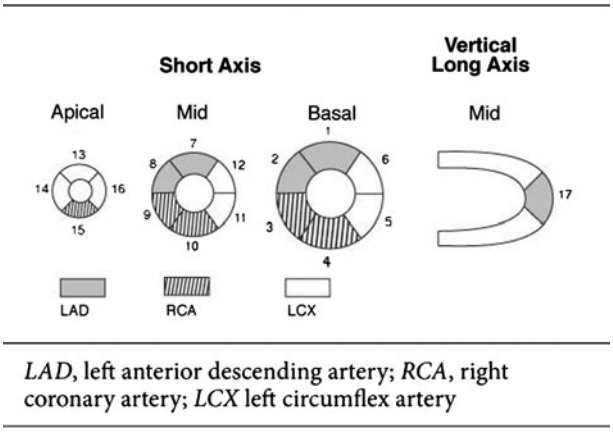

LAD, left anterior descending artery; *RCA*, right coronary artery; *LCX* left circumflex artery

Figure 2. SPECT myocardial perfusion imaging: coronary artery territories.

compared to adjacent activity without the appearance of wall thinning, moderate defects demonstrate wall thinning, and severe defects are those that approach background activity. Defect extent may be qualitatively described as small, medium, or large. In semiquantitative terms, small represents less than 10%, medium represents 10-20%, and large represents greater than or equal to 20% of the LV. Alternatively, defect extent may also be estimated as a fraction such as the ''basal one half'' or ''apical one-third'' of a particular wall or as extending from the base to the apex. Defects whose severity and extent do not change between stress and rest images are categorized as ''fixed'' or ''nonreversible.'' When perfusion defects are more severe and/or extensive on stress compared to resting images, a qualitative description of the degree of reversibility is required.

5.4.6.2. Semiquantitative. In addition to the qualitative evaluation of perfusion defects, it is recommended that the physician also apply a semiquantitative segmental scoring system. This approach standardizes the visual interpretation of scans, reduces the likelihood of overlooking significant defects, and provides an important semiquantitative index that is applicable to diagnostic and prognostic assessments. The QA Committee of the American Society of Nuclear Cardiology has considered several models for segmentation of the perfusion images and has previously recommended either a 17- or 20-segment model for semiquantitative visual analysis. In order to facilitate consistency of nomenclature with other imaging modalities, the 17-segment model is preferred and the 20-segment model should no longer be used.[72,73]

The myocardial segments may be roughly assigned to coronary arterial territories as indicated in Fig. 2 as long as the reader realizes that there can be considerable variation among patients in the inferior and inferolateral segments of the LV due to the variable extent of the circumflex and right coronary artery territories.

The use of a scoring system provides a reproducible semiquantitative assessment of defect severity and extent. A consistent approach to defect severity and extent are clinically important because both variables contain independent prognostic information. Points are assigned to each segment according to the perceived count density of the segment.

In addition to individual scores, it has been recommended that summed scores be calculated. The summed stress scores equals the sum of the stress scores of all the segments and the summed rest score equals the sum of the resting scores (or redistribution scores) of all the segments. The summed difference score equals the difference between the summed stress and the summed resting (redistribution) scores and is a measure of perfusion defect reversibility reflecting inducible ischemia. In particular, the summed stress score has been shown to have significant prognostic power,[74] although the resting perfusion data provide incremental prognostic information as well.[75,76] Before scoring, it is necessary for the interpreting physician to be familiar with the normal regional variation in count distribution of myocardial perfusion SPECT in men and women.

5.4.6.3. Quantitative. Quantitative analysis is useful to supplement visual interpretation.[77,78] Most techniques of quantitative analysis are based on radial plots of short-axis slices, and analyze the apex separately. These plots are then normalized to allow comparison to a normal gender-specific database. Defect severity can be defined based on the patient's regional myocardial tracer activity compared to the mean regional activity of a normal database. Quantitation of the stress perfusion is compared to the resting perfusion to assess the extent and severity of ischemia. It is customary to use separate normal databases specific to the patient's gender as well as the perfusion agent used. This quantitative analysis is typically displayed as a ''bulls-eye'' or polar plot. The quantitative programs are effective in providing an

objective interpretation that is inherently more reproducible than visual analysis, eliminates the variability of the appearance of a defect when viewed in different media (with different gammas) and different translation tables, and is particularly helpful in identifying subtle changes between two studies in the same patient.[79-81] Quantitative analysis also serves as a guide for the less experienced observer who may be uncertain about normal variations in uptake. Quantitative programs are not sophisticated enough to unequivocally differentiate perfusion defects from artifact in all cases. Because of imaging artifacts and the underestimation of ischemia with current SPECT perfusion tracers, there will always be difficulty in distinguishing normal subjects and patients with mild perfusion defects. Quantitative analysis should only be used as an adjunct to, and not a substitute for, visual analysis. Defect extent may be quantitatively expressed as a percentage of the entire left ventricle or as a percentage of individual vascular territories, the latter being less reliable because of the normal variations in coronary anatomy. Defect severity may be quantitatively expressed as the number of standard deviations by which the segment varies from the normal range for that particular segment. Defect reversibility may also be expressed as a percentage of the entire left ventricle or of a vascular territory.

5.4.7. Reversibility. Reversibility of perfusion defects may be categorized qualitatively as partial or complete, the latter being present when the activity in the defect returns to a level comparable to surrounding normal myocardium. The semiquantitative scoring system may be used to define reversibility as a $\geq$2-grade improvement or improvement to a score of 1. Reversibility on a quantitative polar or on 3D displays will depend on the particular software routine in use and the normal reference databases used in the program. Areas of reversibility are typically described by pixels that improve to $<$2.5 SDs from the normal reference redistribution or resting database. How many pixels have to improve for reversibility to be deemed present is arbitrary.

So-called ''reverse redistribution'' may be seen in stress-delayed thallium imaging sequences and has been described in rest-delayed technetium sestamibi sequences.[82] Reverse redistribution refers to segments with decreased or normal intensity on the initial set of images that show even less relative intensity on the delayed images. The interpretation of the finding remains controversial, and in most cases this image pattern is the result of slightly more severe attenuation artifact on low-dose resting images compared to high-dose stress images. Reverse redistribution pattern has also been reported to occur in myocardial segments with a mixture of viable and nonviable myocardium that are supplied by patent infarct-related arteries.[83]

5.5. Gated Myocardial Perfusion SPECT

Because of the comparatively low additional cost and substantial benefit of the information obtained, gated studies of ventricular function should be a routine part of myocardial perfusion SPECT.[41,42] A systematic approach to the display and interpretation of the ventricular function derived from gated SPECT is important.

5.5.1. Gated SPECT display. Multiple ventricular slices should be displayed for visual assessment of regional wall motion and systolic wall thickening. At a minimum, a display of apical and mid-basal short-axis, a mid-ventricular horizontal long-axis, and a mid-ventricular vertical long-axis slice should be viewed. Ideally, the software should allow the user to scroll through any of the slices in any axis in cine mode. Each view should be normalized to the series of end-diastolic to end-systolic slices to maintain the apparent count density changes during the cardiac cycle that reflect myocardial wall thickening. When available, software algorithms that automatically define epicardial and endocardial borders and calculate ventricular volumes and EF should be applied. Regional wall motion should be interpreted with a gray scale display. When computer edge analysis software is available, the physician may choose to analyze wall motion by use of the assigned endocardial and epicardial contours, but reference should also be made to the wall motion without computer-derived edges. Regional wall thickening may be analyzed in gray scale or in a suitable color scheme, although color displays may make it easier to appreciate changes in count intensity.

5.5.2. Gated SPECT QC. All the QA procedures for routine SPECT are applicable to gated SPECT with the addition of the evaluation of the adequacy of the electrocardiographic (ECG) gate.[43] The most common manifestation of poor gating is the appearance of a flashing pattern on the rotating planar projection images that results from count loss in the later frames. Ideally, a heart-rate histogram should also be viewed to verify beat length uniformity. Inspecting the time-volume curve is particularly useful since gating errors may distort the curve. Another important aspect of QC is a visual or quantitative determination that the number of counts acquired in each frame of the gated study was adequate for assessment of function. Software that collects all counts into a separate bin for the summed image can minimize the effect that gating errors have on the summed image.

5.5.3. Gated SPECT: regional wall motion and thickening. Regional wall motion should be analyzed by the use of standard nomenclature: normal, hypokinesis, akinesis, and dyskinesis. Hypokinesis may be further qualified as mild, moderate, or severe. A semiquantitative scoring system is recommended where 0

is normal, 1 is mild hypokinesis, 2 is moderate hypokinesis, 3 is severe hypokinesis, 4 is akinesis, and 5 is dyskinesis.

This is comparable to the 5-point scoring system used in both contrast and radionuclide ventriculography. As in any assessment of regional ventricular function, one must be cognizant of expected normal and abnormal variations such as the reduced wall excursion at the base compared with the apex, the greater excursion of the basal lateral wall compared with the basal septum, and paradoxical septal motion, which may result from left bundle branch block, post pericardiotomy, or RV pacing.

Normal myocardial wall thickness is below the spatial resolution of currently available SPECT systems. Because of the ''partial volume effect,'' regional wall thickening can be estimated by the count increase from end diastole to end systole. It is more difficult to visually assess the severity of abnormality of myocardial wall thickening than it is to visually estimate abnormalities of wall motion. However, the evaluation of thickening with gated perfusion SPECT lends itself to quantitation because it is characterized by count changes.

Wall motion and wall thickening are generally concordant. The principle exception to this occurs in patients who have undergone cardiac surgery where septal wall motion is frequently abnormal (paradoxical), but there is normal wall thickening. Rather than separately scoring wall motion and wall thickening, it is commonly accepted to incorporate the two findings into a single score while noting the presence of discordance in wall motion and wall thickening when it occurs. In addition to noting LV wall motion, wall thickening, and EF, the function of the RV should also be noted. Quantitative normal databases are available for assessment of regional wall thickening.

5.5.4. Left ventricular ejection fraction and volume. LVEF and LV and RV chamber sizes should routinely be evaluated qualitatively.[84] EF may be categorized as normal, mildly, moderately, or severely reduced. Volume may be categorized as normal, mildly, moderately, or severely increased. Alternatively, LVEF and end-diastolic and end-systolic volumes may be calculated with geometric models applied to the reconstructed data set. Several software routines that correlate well with contrast and other radionuclide measurements are commercially available.

5.5.5. Integration of perfusion and function results. The results of the perfusion and gated SPECT data sets should be integrated into a final interpretation. The wall motion is particularly helpful in distinguishing nonreversible (fixed) perfusion defects due to prior myocardial infarction from nonreversible defects due to attenuation artifacts. Fixed perfusion defects that do not show a corresponding abnormality of wall motion or myocardial systolic thickening are more likely to be due to artifacts, especially if the clinical data do not support prior infarction.[58] The finding of normal regional wall motion and myocardial systolic thickening cannot be used to exclude ischemia in patients with reversible perfusion defects.

5.6. Myocardial Viability

5.6.1. Qualitative assessment. The assessment of myocardial viability is a complex issue made even more difficult by the lack of consensus in the literature of the precise meaning of the term viability—whether it refers merely to the absence of scar or requires improvement in wall motion after revascularization. It is, however, clear that the quantitative uptake of radionuclides such as Tl-201 and the available technetium agents does correlate with myocardial viability as defined by postrevascularization improvement in both tracer uptake and regional function. Myocardial segments with normal or mildly reduced tracer uptake at rest or on delayed imaging almost invariably prove to be viable. The majority of myocardial segments in which there is unequivocal improvement of uptake on either redistribution or resting images also prove to be viable. The presence of inducible ischemia implies the presence of viability and predicts a high likelihood of improvement with revascularization. The more difficult challenge for the single photon assessment of viability is in segments with severely reduced tracer uptake on resting images.

5.6.2. Semiquantitative assessment. The semiquantitative scoring system described above may be used to assess viability as follows. As a general rule, segments with rest, reinjection, or redistribution scores of 0 (normal perfusion) and 1 (slight reduction in counts) are considered viable. Segments with rest, redistribution, or reinjection scores of 2 (moderately decreased perfusion) likely represent a combination of viable and nonviable myocardium, and segments with scores of 3 are generally felt to be nonviable. Segments with scores of 4 are considered nonviable.

5.6.3. Quantitative assessment. An alternate and perhaps more rigorous approach to the assessment of the viability of any segment is the quantitative determination of ischemic-to-normal ratios. ROIs may be placed over the segment in question and over the most normal segment of the myocardium in that particular series of images. The analysis should be applied to the resting images for technetium images or to the resting, redistribution, or reinjection images for thallium. When this approach is used, one must take into account the normal count variations such as the relatively reduced counts in the normal inferior wall.

Segments with ratios <.30 are considered nonviable. Areas with ratios greater than .50 are considered viable, whereas areas with ratios of .30 to .50 are considered equivocal for viability. As indicated above for the semiquantitative approach, such regions require additional data such as wall motion of the region, stress perfusion in the region (ischemia implies viability), the change in perfusion or wall motion after nitroglycerin, the response of regional function to low-dose dobutamine, or myocardial metabolic imaging with F-18 fluorodeoxyglucose (FDG).

It is also important to recognize that viability of a given segment does not necessarily equate to improvement in clinical outcome after revascularization unless enough segments that are viable are available. The critical number of segments necessary to justify revascularization strategies has not been adequately defined, and will depend in part on the patient's comorbidities and the risks for adverse short-term outcome with revascularization.

5.7. Modification of Interpretation by Relevant Clinical Information

Due to imperfections in the technology as well as the gradual impairment of coronary blood flow as stenoses become hemodynamically significant, there will always be overlap between the perfusion patterns of normal subjects and patients with mildly abnormal myocardial perfusion. When uncertainty exists, it is helpful to incorporate other clinical information (e.g., symptoms, risk factors, ST-segment changes, exercise tolerance) to help the referring physician make the most appropriate management decisions for the patient. Homogeneous perfusion images of patients who have other markers of severe ischemia, such as marked ST-segment changes, should be carefully evaluated for adjunctive markers of ischemia such as increased stress:rest LV cavity ratio (TID) or increased lung uptake (particularly with thallium) in order to identify those patients with balanced ischemia due to multi-vessel coronary artery disease. The majority of artifacts encountered will produce mild defects; therefore moderate or severe defects, in the absence of severe artifact on rotating planar projection images, should be considered as reflecting pathology. Finally, it needs to be understood that not all abnormalities of myocardial perfusion are caused by obstructive epicardial coronary artery disease (CAD).

5.8. Clinical Interpretation of AC SPECT Studies

The interpretation of AC SPECT myocardial perfusion images follows a similar approach to that used for uncorrected myocardial perfusion images, but there are differences and these should be taken into account in order to obtain good results. The normal distributions of perfusion tracer uptake are significantly different with AC compared to uncorrected studies, and because of this, it is important that the interpreting physician have available and learn databases of normal tracer distribution(s). Although from system to system these normal distributions are generally relatively similar, there can be differences that are dependent on the geometry of the imaging system, acquisition protocol, and processing algorithms.[60] There can also be differences in normal distribution(s) related to patient gender and ventricular volume. The interpreting physician must be aware of these differences if they exist for their imaging system(s) and take them into account on a patient-by-patient basis when assessing clinical studies.

AC SPECT studies generally have more uniform regional activity in the anterior, septal, inferior, and lateral walls, but mild reductions in apical and distal anterior activity are typical of the normal AC image distribution. This apical and distal anterior activity reduction is similar to that seen with PET MPI. This finding becomes more prominent when resolution recovery and scatter correction are included in the AC processing workflow and is often more prominent in patients with larger hearts. In low-likelihood normal patients, this reduction in distal activity is generally more prominent in men than women as men generally have larger hearts. If men and women with similar heart sizes are compared, the difference disappears. In general, the success of AC SPECT appears related to the diligence of the clinical laboratory in following recommended procedures for image acquisition, reconstruction, QA, display, and quantification. Likewise, quantification and display programs without appropriate normal AC databases should not be used for quantification as spurious results will occur.

QA requirements are more demanding with AC than non-AC images and should be carefully assessed for each patient study. Artifacts due to movement, either respiration or patient movement, misregistration, and extracardiac radiotracer uptake can be amplified by the iterative algorithms that are employed in AC reconstructions and processing. The quality and registration of the attenuation maps (or mu maps) with the emission image data are additional key factors that must be ensured, and if they cannot be ensured, the associated AC images should read with greater caution. QA tools to aid these assessments of registration and mu map quality are still not uniformly available, but this should improve in the near future.

For the clinical interpretation of AC SPECT myocardial perfusion images, it is recommended that AC and non-AC images be displayed side-by-side with displays

of the normal activity distribution(s) and their variance distribution available as required for comparison. This requires the availability of normal databases specific for the imaging device, imaging protocol, and processing approach employed clinically. Extracardiac activity especially when combined with respiratory and or patient movement can introduce artifacts and or normalization errors that may require renormalization or abandonment of the AC images altogether. Artifactual reductions in activity most often affecting the apparent anterior and/or lateral wall perfusion tracer uptake can occur when there is misregistration of SPECT and mu map images such that the myocardial activity from the SPECT images is matched with the relatively low attenuation coefficients for adjacent lung tissue in the mu maps. Some attenuation correction-capable SPECT systems acquire the SPECT and the transmission image data sequentially rather than simultaneously. If there is a change in position of arm(s) or breasts between emission and transmission imaging even though there may be perfect registration of the heart in the emission and transmission images, there can be artifactual defects introduced into the SPECT perfusion images by the misregistration of tissues outside the thorax.

The SPECT/CT systems that have become available recently require sequential emission and transmission imaging with a change in bed position between acquisitions. Although the quality of the mu maps with these systems will consistently far exceed the quality of sealed source transmission system mu maps, the greatly improved resolution of the mu maps they provide make it even more important that registration of emission and transmission reconstructions be exact to less than one pixel tolerance.

5.9. Reporting of SPECT Myocardial Perfusion Scan Results

5.9.1. Principles of reporting. The reporting of SPECT myocardial perfusion imaging should provide critical information to the referring practitioner in a comprehensive but clinically relevant manner. The data elements contained in the report should be based on the common lexicon for cardiac imaging, whenever possible.[85] These data elements were developed as part of a multisocietal effort to promote harmonization across imaging modalities and to permit development of quality metrics in imaging. The details regarding exact definitions for each data field are beyond the scope of these guidelines, but have been well-defined.

The final report may be used for a variety of purposes beyond the conveyance of information to the referring clinician, including billing, quality improvement, teaching, and research.[73,86] As such, standardization of the report improves communication and integration of data and through structured reporting, information is conveyed in a coherent and predictable format. The key principles of structured reporting have been elucidated[86] as well as the need for balance, such as consistency vs flexibility. Vendors of reporting system software and electronic health record systems are encouraged to follow and promote accepted standards and to facilitate the adoption of such system. Of note, both ASNC and the American College of Cardiology support mandatory the use of structured reporting.

The principals of structured reporting and a detailed description of data elements were recently published by ASNC, serving to update prior reporting documents.[73] These guidelines for structured reporting detail all report components and their definitions, as do this document, and specify whether specific elements must be contained in the report (required), are recommended to be in the report, or are optional elements. These guidelines, while not comprehensive should serve as a laboratory standard for all forms of reports. Furthermore, these guidelines are intended to serve as the basis for a standard for laboratory accreditation.

Finally, timeliness is an important aspect of reporting, as the results of SPECT imaging must be conveyed to the referring clinician in a reasonable time frame. High-risk findings should be communicated as soon as possible by means of telephone or electronic communication, certainly on the same day of interpretation. All reports should be completed within 24 hours of study acquisition and the final report made available within 48 hours.[87]

5.9.2. Components of SPECT myocardial perfusion imaging reports.

5.9.2.1. Subject information. The age and/or date of birth, gender, height, weight, body surface area, race and ethnicity should be included in the report because they may directly affect the image results and interpretation. For medical records purposes, a unique patient identifier should be included. Pertinent medications that may influence the results should be included.

5.9.2.2. Type of study. The imaging protocol should be specified, including the radiopharmaceutical and dose, imaging technique (gated vs ungated; supine and/or prone), imaging sequence (stress/4-hour redistribution, 1-day or 2-day rest/stress or stress/rest, and so on), and a specific statement about whether images were or were not corrected for attenuation.

5.9.2.3. Date. The date(s) of the study and the date of the report should be included within the final report.

5.9.2.4. Referring clinician. The name of the referring physician should be included on the report.

5.9.2.5. Indication for study. Placing the indication for the study in the report helps focus the

interpreting physician on the clinical question raised by the ordering physician and may be subsequently important for reimbursement issues. The primary reason should be chosen from the options available for all cardiac imaging procedures.

5.9.2.6. ECG findings. Inclusion of ECG findings that may have a direct bearing on the study interpretation should be included such as the presence of left bundle branch block or LV hypertrophy, rhythm, and resting ST segment abnormalities.

5.9.2.7. Summary of stress data. The type of stress (bicycle or treadmill) and the protocol should be identified (e.g., Bruce, modified Bruce, Naughton, manual). For pharmacologic stress, the agent, route of administration, and dose should be indicated. Additionally, the reason why a pharmacologic test was performed, as opposed to exercise should be included. The reason for test termination should be noted. All symptoms experienced by the patient during the stress (e.g., chest pain, dyspnea, claudication, dizziness) should be mentioned.

If a separate stress test report is generated, a practice which is discouraged, then the stress variables that could impact on the perfusion study quality or findings should be included in the perfusion scan report. At a minimum, the report should include the total exercise duration, maximal heart rate and percent of predicted maximum heart rate, resting and maximal blood pressure achieved and workload achieved (estimated metabolic equivalents), and the magnitude (in millimeters) and location of any ST-segment deviation.

A combined report for both the exercise or pharmacologic study and the perfusion results is recommended and should include specific details related to the stress test, such as time of onset, duration and exact ECG leads with ST-segment changes, the type of chest pain (typical, atypical, and nonanginal) and its severity (mild, moderate, and severe), and the presence of arrhythmia.

5.9.2.8. Overall study quality. First, the adequacy of stress should be noted, such that the patient has achieved an adequate heart-rate response to exercise or an adequate response to pharmacologic stress. A statement about the quality of the perfusion study is helpful as it alerts the physicians using the report to any shortcomings that might reduce the accuracy of the data and their interpretation.

5.9.2.9. Results–perfusion. Perfusion defects should be defined in terms of extent, severity, and location for all abnormalities. Each defect should be characterized as either ischemia, scar, or mixed. Localization should be based on the 17-segment model and its attendant nomenclature.[72] The severity of abnormalities should be described as mild, moderate, or severe. Finally, the extent of the defect should be defined based on the number of abnormal segments: small (1-2 segments), moderate (3-4 segments), or large ($\geq$5 segments).

5.9.2.10. Results–function. Overall LV function should be described as normal, hyperdynamic, or with mild, moderate, or severe dysfunction. Regional abnormalities should be also noted and based on the 17 segment model for localization. The quantitative left ventricular ejection fraction should be included.

5.9.2.11. Conclusions–general. The final interpretation of the scan should obviously reflect the reader's impression as to whether the scan is normal or abnormal. The scan may also be found to be equivocal. Other terminology, such as ''probably'' or ''possibly,'' should be avoided. Correlation with other imaging studies should be included, as well as a comparison to prior SPECT studies.

5.9.2.12. Conclusions–diagnosis and prognosis of CAD. The probability of CAD may be determined with available algorithms that use the prescan likelihood of CAD. The perfusion data are then added to the model to produce a post-test probability of CAD, which may be reported. When CAD is known to be present, the likelihood of stress-induced ischemia may be reported instead of the likelihood of significant CAD.

5.9.2.13. Signature. All reports must be signed, either by hand or electronically by the interpreting physician. A stamped signature is not sufficient.

5.9.2.14. Date of report. The date of interpretation, as well as when the final report is signed, must be part of the final report.

Acknowledgments

Dr. Robert Hendel receives grant support from GE Healthcare, is on the Speakers' Bureau for Astellas Pharma US, and serves on the Advisory Boards for PGx Health, Astellas Pharma US, UnitedHealthcare, and GE Healthcare. Dr. Donna Polk serves on the Data Safety Monitoring Board for Lantheus. Dr. Dennis Calnon serves on the Research Steering Committee for PGx Health. Dr. Christopher Hansen receives grant support from Digirad and is a stock shareholder of General Electric. The authors have no conflicts of interest to disclose except as noted above.

APPENDIX

See Tables 12-17

Table 12. Patient protocol: same-day rest-stress Tc-99m acquisition

	Rest study	Stress study	
Dose	8-12 mCi	24-36 mCi	Standard
Position	Supine	Supine	Standard
	Prone	Prone	Optional
	Upright/semiupright	Upright/semiupright	Optional
Delay time (intervals)			
Injection → imaging	30-60 minutes	15-60 minutes	Standard
Rest → stress		30 minutes to 4 hours	Standard
Acquisition protocol			
Energy window	15 -20% symmetric	Same	Standard
Collimator	LEHR	Same	Preferred
Orbit	180° (45° RAO to 45° LPO)	Same	Preferred
Orbit type	Circular	Same	Standard
	Noncircular	Same	Standard
Pixel size	6.4 ± .4 mm	Same	Standard
Acquisition type	Step and shoot	Same	Standard
	Continuous	Same	Optional
Number of projections	60-64	Same	Standard
Matrix	64 × 64	Same	Standard
Time/projection	25 s	20 s	Standard
ECG gated	Optional	Standard	Preferred
Frames/cycle	8	8	Standard
	16	16	Optional
R-to-R window	100%	100%	Preferred

RAO, Right anterior oblique; *LPO*, left posterior oblique.

Table 13. Patient protocol: same-day stress-rest Tc-99m acquisition

Parameter	Stress study	Rest study	
Dose	8-12 mCi	24-36 mCi	Standard
Position	Supine	Supine	Standard
	Prone	Prone	Optional
	Upright/semiupright	Upright/semiupright	Optional
Delay time (intervals)			
Injection → imaging	15-60 minutes	30-60 minutes	Standard
Stress → rest		30 minutes to 4 hours	Standard
Acquisition protocol			
Energy window	15-20% symmetric	Same	Standard
Collimator	LEHR	Same	Preferred
Orbit	180° (45° RAO to 45° LPO)	Same	Preferred
Orbit type	Circular	Same	Standard
	Noncircular	Same	Standard
Pixel size	6.4 ± .4 mm	Same	Standard
Acquisition type	Step and shoot	Same	Standard
	Continuous	Same	Optional
Number of projections	60-64	Same	Standard
Matrix	64 × 64	Same	Standard
Time/projection	25 s	20 s	Standard

Table 13 continued

Parameter	Stress study	Rest study	
ECG gated	Optional	Standard	Preferred
Frames/cycle	8	8	Standard
	16	16	Optional
R-to-R window	100%	100%	Preferred

RAO, Right anterior oblique; *LPO*, left posterior oblique.

Table 14. Patient protocol: two-day stress Tc-99m acquisition

Parameter	Stress study	Rest study	
Dose	30 mCi	30 mCi	Standard
Position	Supine	Supine	Standard
	Prone	Prone	Optional
Delay time (intervals)			
Injection → imaging	15-60 minutes	30-60 min	Standard
Acquisition protocol			
Energy window	15-20% symmetric	Same	Standard
Collimator	LEHR	Same	Preferred
Orbit	180° (45° RAO to 45° LPO)	Same	Preferred
Orbit type	Circular	Same	Standard
	Noncircular	Same	Standard
Pixel size	6.4 ± .4 mm	Same	Standard
Acquisition type	Step and shoot	Same	Standard
	Continuous	Same	Optional
Number of projections	60-64	Same	Standard
Matrix	64 × 64	Same	Standard
Time/projection	20 s	20 s	Standard
ECG gated	Standard	Standard	Preferred
Frames/cycle	8	8	Standard
	16	16	Optional
R-to-R window	100%	100%	Preferred

RAO, Right anterior oblique; *LPO*, left posterior oblique.

Table 15. Patient protocol: separate dual-isotope acquisition

Parameter	Rest study	Stress study	
Dose	2.5-3.5 mCi Tl-201	30 mCi Tc-99 m	Standard
Position	Supine	Supine	Standard
	Prone	Prone	Optional
	Upright/semiupright	Upright/semiupright	Optional
Delay time (intervals)			
Injection → imaging	10-15 minutes	15-60 minutes	Standard
Rest → stress		No delay	Standard
Acquisition protocol			
Energy window	25-30% symmetric 70 keV 20% symmetric 167 keV	15-20% symmetric 140 keV	Standard

Table 15 continued

Parameter	Rest study	Stress study	
Collimator	LEHR	Same	Preferred
Orbit	180° (45° RAO to 45° LPO)	Same	Preferred
Orbit type	Circular	Same	Standard
	Noncircular	Same	Standard
Pixel size	6.4 ± .4 mm	Same	Standard
Acquisition type	Step and shoot	Same	Standard
	Continuous	Same	Optional
Number of projections	32-64	60-64	Standard
Matrix	64 × 64	Same	Standard
Time/projection	40 s (32 fr) 25 s (64 fr)	20 s	Standard
ECG gated	Optional	Standard	Preferred
Frames/cycle	8	8	Standard
	16	16	Optional
R-to-R window	100%	100%	Preferred

RAO, Right anterior oblique; *LPO*, left posterior oblique.

Table 16. Patient protocol: stress/redistribution Tl-201 acquisition

Parameter	Stress study	Redistribution rest study	
Dose	2.5-3.5 mCi Tl-201	Not applicable	Standard
Position	Supine	Supine	Standard
	Prone	Prone	Optional
	Upright/semiupright	Upright/semiupright	Optional
Delay time			
Injection → imaging	10-15 minutes*	Not applicable	Standard
Stress → rest		3-4 hours	Standard
Acquisition protocol			
Energy window	30% Symmetric, 70 keV	Same	Standard
	20% Symmetric, 167 keV		
Collimator	LEAP	Same	Preferred
Orbit	180° (45° RAO to 45° LPO)	Same	Preferred
Orbit type	Circular	Same	Standard
	Noncircular	Same	Standard
Pixel size	6.4 ± .4 mm	Same	Standard
Acquisition type	Step and shoot	Same	Standard
	Continuous	Same	Optional
Number of projections	32-64	Same	Standard
Matrix	64 × 64	Same	Standard
Time/projection	40 s (32 fr) 25 s (64 fr)	40 s (32 fr) 25 s (64 fr)	Standard

Table 17. Patient protocol: stress/reinjection/redistribution Tl-201 acquisition

Parameter	Stress study	Reinjection	(Redistribution) rest study	
Dose	2.5–3.5 mCi	1.0–1.5 mCi	Not applicable	Standard
Position	Supine		Supine	Standard
	Prone		Prone	Optional
	Upright/semiupright		Upright/semiupright	Optional
Delay time (intervals)				
Injection → imaging	10–15 minutes		Not applicable	Standard
Stress → redistribution			3–4 hours	Standard
Reinjection → imaging (MI)			20–30 minutes	Standard
24-h imaging				Optional
Acquisition protocol				
Energy window	30% Symmetric, 70 keV 20% symmetric, 167 keV		Same	Standard
Collimator	LEAP		Same	Preferred
Orbit	180° (45° RAO to 45° LPO)		Same	Preferred
Orbit type	Circular		Same	Standard
	Noncircular		Same	Standard
Pixel size	6.4 ± .4 mm		Same	Standard
Acquisition type	Step and shoot		Same	Standard
	Continuous		Same	Optional
Number of projections	32–64		Same	Standard
Matrix	64 × 64		Same	Standard
Time/projection	40 s (32 fr) 25 s (64 fr)		40 s (32 fr) 25 s (64 fr)	Standard

References

1. Kennedy JA, Yosilevsky G, Przewloka K, Israel O, Frenkel A. 3D spatial resolution map and sensitivity characterization of a dedicated cardiac CZT SPECT camera [abstract]. J Nucl Med 2009;50:107.
2. Garcia EV, Tsukerman L, Keidar Z. A new solid state, ultra fast cardiac multi-detector SPECT system [abstract]. J Nucl Cardiol 2008;15:S3.
3. Gambhir SS, Berman DS, Ziffer JA, et al. A novel high-sensitivity rapid-acquisition single-photon cardiac imaging camera. J Nucl Med 2009;50:635-43.
4. Bushberg JT, Seibert JA, Leidholt EM, Boone JM. The essential physics of medical imaging. Baltimore, MD: Williams & Wilkins; 1994.
5. Cherry SR, Sorenson JA, Phelps ME. Physics in nuclear medicine. 3rd ed. Philadelphia, PA: Elsevier Science; 2003.
6. Cullom SJ. Principles of cardiac SPECT imaging. In: DePuey EG, Berman DS, Garcia EV, editors. Cardiac SPECT. 2nd ed. Philadelphia, PA: Lippincott, Williams & Wilkins; 2001. p. 3-16.
7. Shepp LA, Vardi Y. Maximum likelihood reconstruction for emission tomography. IEEE Trans Med Imaging 1982;1:113-22.
8. Hudson HM, Larkin RS. Accelerated image reconstruction using ordered subsets of projection data. IEEE Trans Med Imaging 1994;13:601-9.
9. Bowsher JE, Floyd CE. Treatment of Compton scattering in maximum likelihood, expectation-maximization reconstructions of SPECT images. J Nucl Med 1991;32:1285-91.
10. Xaio J, de Wit TC, Staelen SG, Beekman FJ. Evaluation of 3D Monte Carlo-based scatter correction for 99mTc cardiac perfusion SPECT. J Nucl Med 2006;47:1662-9.
11. Daou D, Pointurier I, Coaguila C, et al. Performance of OSEM and depth-dependent resolution recovery algorithms for the evaluation of global left ventricular function in 201Tl gated myocardial perfusion SPECT. J Nucl Med 2003;44:155-62.
12. DiFilippo FP, Abreu SH, Majmundar H. Collimator integrity. J Nucl Cardiol 2006;13:889-91.
13. O'Connor MK. Instrument- and computer-related problems and artifacts in nuclear medicine. Semin Nucl Med 1996;26: 256-77.
14. Lau YH, Hutton BF, Beekman FJ. Choice of collimator for cardiac SPECT when resolution compensation is included in iterative reconstruction. Eur J Nucl Med 2001;28:39-47.
15. Devito RP, Haines EJ, Domnanovitch JR, inventors. Mosaic Imaging Technology, Inc. Non-orbiting tomographic imaging system. US Patent 6242743, June 5, 2001.
16. Sharir T, Ben-Haim S, Merzon K, et al. High-speed myocardial perfusion imaging initial clinical comparison with conventional dual detector anger camera imaging. J Am Coll Cardiol Imaging 2008;1:156-63.
17. Hawman PC, Haines EJ. The cardiofocal collimator: A variable-focus collimator for cardiac SPECT. Phys Med Biol 1994;39:439-50.
18. Hasegawa B, Kirch D, Stern D, et al. Single-photon emission tomography with a 12-pinhole collimator. J Nucl Med 1982; 23:606-12.

19. Steele PP, Kirch DL, Koss JE. Comparison of simultaneous dual-isotope multipinhole SPECT with rotational SPECT in a group of patients with coronary artery disease. J Nucl Med 2008;49:1080-9.
20. Herzog BA, Beuchel RR, Katz R, et al. Nuclear myocardial perfusion imaging with cadmium-zinc-telluride detector technique: Optimized protocol for scan time reduction. J Nucl Med 2010;51:46-51.
21. Shin JH, Pokharna HK, Williams KA, Mehta R, Ward RP. SPECT myocardial perfusion imaging with prone-only acquisitions: Correlation with coronary angiography. J Nucl Cardiol 2009;16: 590-6.
22. Erlandsson K, Kacperski K, van Gramberg D, Hutton BF. Performance evaluation of D-SPECT: A novel SPECT system for nuclear cardiology. Phys Med Biol 2009;54:2635-49.
23. Nichols KG, Galt JR. Quality control for SPECT imaging. In: DePuey EG, Berman DS, Garcia EV, editors. Cardiac SPECT imaging. 2nd ed. Philadelphia, PA: Lippincott Williams & Wilkins; 2001. p. 17-40.
24. National Electrical Manufacturers Association. NEMA Standards Publication NU 1-2007: Performance measurements of scintillation cameras. Washington, DC: National Electrical Manufacturers Association; 2007.
25. Esser PD, Graham LS. A quality control program for nuclear medicine cameras. In: Henkin RE, editor. Nuclear medicine. 2nd ed. Philadelphia, PA: Mosby; 2006. p. 246-56.
26. DePuey EG. How to detect and avoid myocardial perfusion SPECT artifacts. J Nucl Med 1994;35:699-702.
27. Galt JR, Faber T. Principles of single photon emission computed tomography (SPECT) imaging. In: Christian PE, Bernier DR, Langan JK, editors. Nuclear medicine and PET: Technology and techniques. St. Louis: Mosby; 2003. p. 242-84.
28. Cerqueira MD, Matsuoka D, Ritchie JL, Harp GD. The influence of collimators on SPECT center of rotation measurements: Artifact generation and acceptance testing. J Nucl Med 1988;29:1393-7.
29. Hines H, Kayayan R, Colsher J, et al. National Electrical Manufacturers Association recommendation for implementing SPECT instrumentation quality control. J Nucl Med 2000;41:383-9.
30. Greer KL, Jaszczak RJ, Coleman RE. An overview of a camera-based SPECT system. Med Phys 1982;9:455-63.
31. American College of Radiology. ACR Web site. http://www.acr.org. Accessed March 2, 2009.
32. American Association of Physicists in Medicine. AAPM Web site. http://www.aapm.org. Accessed March 2, 2009.
33. American Society of Nuclear Cardiology. ASNC imaging guidelines for nuclear cardiology procedures: Introduction of new technology for clinical use. J Nucl Cardiol 2009;16:166.
34. Chang SM, Nabi F, Xu J, Raza U, Mahmarian JJ. Normal stress-only versus standard stress/rest myocardial perfusion imaging: Similar patient mortality with reduced radiation exposure. J Am Coll Cardiol 2010;55:221-30.
35. Segall GM, Davis MJ. Prone versus supine thallium myocardial SPECT: A method to decrease artifactual inferior wall defects. J Nucl Med 1989;30:548-55.
36. Kiat H, Van Train KF, Friedman JD, Germano G, Silagan G, Wang FP, et al. Quantitative stress-redistribution thallium-201 SPECT using prone imaging: Methodologic development and validation. J Nucl Med 1992;33:1509-15.
37. Esquerre JP, Coca FJ, Martinez SJ, Guiraud RF. Prone decubitus: A solution to inferior wall attenuation in thallium-201 myocardial tomography. J Nucl Med 1989;30:398-401.
38. Nishina H, Slomka PJ, Abidov A, et al. Combined supine and prone quantitative myocardial perfusion SPECT: Method development and clinical validation in patients with no known coronary artery disease. J Nucl Med 2006;47:51-8.
39. Slomka PJ, Nishina H, Abidov A, et al. Combined quantitative supine-prone myocardial perfusion SPECT improves detection of coronary artery disease and normalcy rates in women. J Nucl Cardiol 2007;14:44-52.
40. Friedman J, Van Train K, Maddahi J, Rozanski A, Prigent F, Bietendorf J, et al. ''Upward creep'' of the heart: A frequent source of false-positive reversible defects during thallium-201 stress-redistribution SPECT. J Nucl Med 1989;30:1718-22.
41. Bateman TM, Berman DS, Heller GV, Brown KA, Cerqueira MD, Verani MS, et al. American Society of Nuclear Cardiology position statement on electrocardiographic gating of myocardial perfusion SPECT scintigrams. J Nucl Cardiol 1999;6:470-1.
42. Cullom SJ, Case JA, Bateman TM. Electrocardiographically gated myocardial perfusion SPECT: Technical principles and quality control considerations. J Nucl Cardiol 1998;5:418-25.
43. DePuey EG, Nichols K, Dobrinsky C. Left ventricular ejection fraction assessed from gated technetium-99m-sestamibi SPECT. J Nucl Med 1993;34:1871-6.
44. Smanio PE, Watson DD, Segalla DL, Vinson EL, Smith WH, Beller GA. Value of gating of technetium-99m sestamibi single-photon emission computed tomographic imaging. J Am Coll Cardiol 1997;30:1687-92.
45. He ZX, Cwajg E, Preslar JS, Mahmarian JJ, Verani MS. Ejection fraction determined by gated myocardial perfusion SPECT with Tl-201 and Tc-99m sestamibi: Comparison with first-pass radionuclide angiography. J Nucl Cardiol 1999;4:412-7.
46. Hansen C. Digital image processing for clinicians, part II: Filtering. J Nucl Cardiol 2002;9:429-37.
47. Hansen CL, Kramer M, Rastogi A. Lower accuracy of Tl-201 SPECT in women is not improved by size-based normal databases or Wiener filtering. J Nucl Cardiol 1999;6:177-82.
48. King MA, Glick SJ, Penney BC, Schwinger RB, Doherty PW. Interactive visual optimization of SPECT prereconstruction filtering. J Nucl Med 1987;28:1192-8.
49. Hansen C. Digital image processing for clinicians, part III: SPECT reconstruction. J Nucl Cardiol 2002;9:542-9.
50. Yester MV. SPECT image reconstruction. In: Henkin RE, editor. Nuclear medicine. 2nd ed. Philadelphia, PA: Mosby; 2006. p. 185-95.
51. Borges-Neto S, Pagnanelli RA, Shaw LJ, et al. Clinical results of a novel wide beam reconstruction methods for shortening scan time of Tc-99m cardiac SPECT perfusion studies. J Nucl Cardiol 2007;14:555-65.
52. DePuey EG, Gadiraju R, Clark J, et al. Ordered subset expectation maximization and wide beam reconstruction ''half-time'' gated myocardial perfusion SPECT functional imaging: A comparison to ''full-time'' filtered backprojection. J Nucl Cardiol 2008;14:547-63.
53. DePuey EG, Bommireddipalli S, Clark J, Thompson L, Srour Y. Wide beam reconstruction ''quarter-time'' gated myocardial perfusion SPECT functional imaging: A comparison to ''full-time'' ordered subset expectation maximum. J Nucl Cardiol 2009;16:736-52.
54. Hansen CL. The role of the translation table in cardiac image display. J Nucl Cardiol 2006;13:571-5.
55. Hansen C. Digital image processing for clinicians, Part I: Basics of image formation. J Nucl Cardiol 2002;9:343-9.
56. Friedman J, Berman DS, Van Train K, Garcia EV, Bietendorf J, Prigent F, et al. Patient motion in thallium-201 myocardial SPECT imaging. An easily identified frequent source of artifactual defect. Clin Nucl Med 1988;13:321-4.
57. Cooper JA, Neumann PH, McCandless BK. Effect of patient motion on tomographic myocardial perfusion imaging. J Nucl Med 1992;33:1566-71.

58. Choi JY, Lee KH, Kim SJ, Kim SE, Kim BT, Lee SH, et al. Gating provides improved accuracy for differentiating artifacts from true lesions in equivocal fixed defects on technetium 99m tetrofosmin perfusion SPECT. J Nucl Cardiol 1998;5:395-401.
59. Ficaro EP, Fessler JA, Shreve PD. et al. Simultaneous transmission/emission myocardial perfusion tomography. Diagnostic accuracy of attenuation-corrected 99mTc-sestamibi single-photon emission computed tomography. Circulation 1996;93:463-73.
60. Fricke H, Fricke E, Weise R, et al. A method to remove artifacts in attenuation-corrected myocardial perfusion SPECT. Introduced by misalignment between emission scan and CT-derived attenuation maps. J Nucl Med 2004;45:1619-25.
61. Grossman GB, Garcia EV, Bateman T, et al. Quantitative Tc-99m sestamibi attenuation-corrected SPECT: Development and multicenter trial validation of myocardial perfusion stress gender-independent normal database in obese population. J Nucl Cardiol 2004;11:263-772.
62. Weiss AT, Berman DS, Lew AS, et al. Transient ischemic dilation of the left ventricle on stress thallium-201 scintigraphy: A marker of severe and extensive coronary artery disease. J Am Coll Cardiol 1987;9:752-9.
63. McLaughlin MG, Danias PG. Transient ischemic dilation: A powerful diagnostic and prognostic finding of stress myocardial perfusion imaging. J Nucl Cardiol 2002;9:663-7.
64. Hansen CL, Sangrigoli R, Nkadi E, Kramer M. Comparison of pulmonary uptake with transient cavity dilation after exercise thallium-201 perfusion imaging. J Am Coll Cardiol 1999;33:1323-7.
65. Hansen CL, Cen P, Sanchez B, Robinson R. Comparison of pulmonary uptake with transient cavity dilation after dipyridamole Tl-201 perfusion imaging. J Nucl Cardiol 2002;9:47-51.
66. Chouraqui P, Rodrigues EA, Berman DS, Maddahi J. Significance of dipyridamole-induced transient dilation of the left ventricle during thallium-201 scintigraphy in suspected coronary artery disease. Am J Cardiol 1990;66:689-94.
67. Abidov A, Bax JJ, Hayes SW, et al. Integration of automatically measured transient ischemic dilation ratio into interpretation of adenosine stress myocardial perfusion SPECT for detection of severe and extensive CAD. J Nucl Med 2004;45:1999-2007.
68. Gill JB, Ruddy TD, Newell JB, et al. Prognostic importance of thallium uptake by the lungs during exercise in coronary artery disease. N Engl J Med 1987;317:1486-9.
69. Wackers FJT. On the bright side. J Nucl Cardiol 2005;12:378-80.
70. Williams KA, Schneider CM. Increased stress right ventricular activity on dual isotope perfusion SPECT: A sign of multivessel and/or left main coronary artery disease. J Am Coll Cardiol 1999;34:420-7.
71. Williams KA, Hill KA, Sheridan CM. Noncardiac findings on dual-isotope myocardial perfusion SPECT. J Nucl Cardiol 2003;10:395-402.
72. Cerqueira MD, Weissman NJ, Dilsizian V, et al. Standardized myocardial segmentation and nomenclature for tomographic imaging of the heart: A statement for healthcare professionals from the Cardiac Imaging Committee of the Council on Clinical Cardiology of the American Heart Association. J Nucl Cardiol 2002;9:240-5.
73. Tilkemeier PL, Cooke CD, Ficaro EP, et al. ASNC imaging guidelines for nuclear cardiology procedures: Standardized reporting of myocardial perfusion images. J Nucl Cardiol 2009;16:165.
74. Hachamovitch R, Berman DS, Shaw LJ, et al. Incremental prognostic value of myocardial perfusion single photon emission computed tomography for the prediction of cardiac death: Differential stratification for risk of cardiac death and myocardial infarction. Circulation 1998;97:535-43.
75. Travin MI. The oft neglected rest study. J Nucl Cardiol 2009;15:739-42.
76. Shaw LJ, Hendel RC, Heller GV, et al. Prognostic estimation of coronary artery disease risk with resting perfusion abnormalities and stress ischemia on myocardial perfusion SPECT. J Nucl Cardiol 2009;15:762-73.
77. Berman DS, Kang X, Van Train KF, et al. Comparative prognostic value of automatic quantitative analysis versus semiquantitative visual analysis of exercise myocardial perfusion single-photon emission computed tomography. J Am Coll Cardiol 1998;32:1987-95.
78. Leslie WB, Tully SA, Yogendran MS, et al. Prognostic value of automated quantification of ^{99m}Tc-sestamibi myocardial perfusion imaging. J Nucl Med 2005;46:204-11.
79. Berman DS, Kang X, Gransar H, et al. Quantitative assessment of myocardial perfusion abnormality on SPECT myocardial perfusion imaging is more reproducible than expert visual analysis. J Nucl Cardiol 2009;16:45-53.
80. Iskandrian AS, Garcia EV, Faber T, Mahmarian JJ. Automated assessment of serial SPECT myocardial perfusion images. J Nucl Cardiol 2009;16:6-9.
81. Mahmarian JJ, Cerqueira MD, Iskandrian AS. Regadenoson induces comparable left ventricular perfusion defects as adenosine: A quantitative analysis from the ADVANCE MPI 2 Trial. J Am Coll Cardiol Img 2009;2:959-68.
82. Takeishi Y, Sukekawa H, Fujiwara S, et al. Reverse redistribution of technetium-99m-sestamibi following direct PTCA in acute myocardial infarction. J Nucl Med 1996;37:1289-94.
83. Weiss AT, Maddahi J, Lew AS, et al. Reverse redistribution of thallium-201: A sign of nontransmural myocardial infarction with patency of the infarct-related coronary artery. J Am Coll Cardiol 1986;7:61-7.
84. Sharir T, Kang X, Germano G, et al. Prognostic value of poststress left ventricular volume and ejection fraction by gated myocardial perfusion SPECT in women and men: Gender-related differences in normal limits and outcomes. J Nucl Cardiol 2006;13:495-506.
85. Hendel RC, Budoff MJ, Cardella JF, et al. ACC/AHA/ACR/ASE/ASNC/NASCI/RSNA/SAIP/SCAI/SCCT/SCMR/SIR key data elements and definitions for cardiac imaging. J Am Coll Cardiol 2009;53:91-124.
86. Douglas PS, Hendel RC, Cummings JE, et al. ACC/ACR/AHA/ASE/ASNC/HRS/MITA/NASCI/RSNA/SAIP/SCCT/SCMR health policy statement on structured reporting in cardiovascular imaging. J Am Coll Cardiol 2009;53:76-90.
87. Hendel RC, Ficaro EP, Williams KA. Timeliness of reporting results of nuclear cardiology procedures. J Nucl Cardiol 2007;14:266.